NIST Technical Note 2046

Estimating real-time infiltration for use in residential ventilation control

Lisa Ng
Stephen Zimmerman
Jeremy Good
Brian Toll
Steven J. Emmerich
Andrew K. Persily

This publication is available free of charge from:
https://doi.org/10.6028/NIST.TN.2046

National Institute of Standards and Technology
U.S. Department of Commerce

NIST Technical Note 2046

Estimating real-time infiltration for use in residential ventilation control

Lisa Ng
Stephen Zimmerman
Steven J. Emmerich
Andrew K. Persily
Engineering Laboratory
Energy and Environment Division
Indoor Air Quality and Ventilation Group

Jeremy Good
Brian Toll
Beetle Management, Inc.

This publication is available free of charge from:
https://doi.org/10.6028/NIST.TN.2046

June 2019

U.S. Department of Commerce
Wilbur L. Ross, Jr., Secretary

National Institute of Standards and Technology
Walter Copan, NIST Director and Undersecretary of Commerce for Standards and Technology

National Institute of Standards and Technology Technical Note 2046
Natl. Inst. Stand. Technol. Tech. Note 2046, 47 pages (June 2019)
CODEN: NTNOEF

This publication is available free of charge from:
https://doi.org/10.6028/NIST.TN.2046

Abstract

Minimum outdoor air ventilation rates specified in standards such as ASHRAE Standard 62.2 are generally based on envelope airtightness, building floor area, geographical location, and number of occupants. In practice, simple on/off controls and operating schedules are most commonly used to maintain the required ventilation rate. Ideally, minimum outdoor ventilation rates should account for unintentional leakage through the building envelope, or "infiltration." ASHRAE Standard 62.2-2016 allows for constant infiltration credit, which reduces the required mechanical ventilation. However, infiltration rates vary based on the indoor-outdoor temperature difference, wind, and system operation. Thus, mechanical systems designed to maintain minimum ventilation rates could operate less, and provide the required minimum rate more reliably, if the real-time infiltration rate was known and used to control the mechanical ventilation rate. Detailed and simplified CONTAM models of two test houses on the campus of the National Institute of Standards and Technology were verified using measured data and then used to simulate real-time infiltration rates. As part of the simulation, these real-time infiltration rates were passed to a theoretical controller that adjusted the mechanical ventilation rate on an hourly basis. Simulated energy use and relative annual occupant exposure for several real-time ventilation control approaches were compared with simulations using a constant ventilation rate. Implementation of the theoretical controllers resulted in annual average energy savings of $68 across both houses and three climates, without a significant increase in annual occupant exposure compared to ventilating continuously at a constant rate. The authors discuss the advantages and limitations of the proposed real-time ventilation control strategies.

Key words

ASHRAE Standard 62.2, CONTAM, energy use, exposure factor, real-time infiltration, residential ventilation, simplified airflow modeling.

Table of Contents

List of Tables

List of Figures

1. Introduction

In ASHRAE Standard 62.2-2016 [1], the minimum required outdoor ventilation rate is determined based on the number of bedrooms and occupiable floor area. An infiltration credit can be used to reduce the required mechanical ventilation in a house. The credit is based on converting an envelope airtightness value to an effective annual infiltration rate using floor area, house height, and location of the house to capture the climatic conditions. The credit is applied to the entire year, even though the actual infiltration rate will be lower or higher than the credit at any given time [2]. Similarly, the infiltration credit does not account for times of the year when the mechanical ventilation plus the actual infiltration rate exceed the outdoor air ventilation requirement, leading to excessive energy use. Application of real-time ventilation control can help achieve the target total ventilation rate on an hourly basis rather than on an annual average basis. This would balance the goals of maintaining acceptable indoor air quality and reducing energy use by avoiding both under- and over-ventilation.

In studies of control strategies to reduce the energy use of mechanical ventilation, carbon dioxide and relative humidity have been used as the control indicator [3]. However, the dynamic nature of infiltration is often not addressed or quantified. One experimental study shut off mechanical ventilation at the highest indoor-outdoor temperature differences to save about 9 % in heating/cooling energy [4]. It was assumed that infiltration would be the greatest under these conditions, which would compensate for the mechanical ventilation system being off. While greater indoor-outdoor temperature differences do result in higher infiltration rates, the infiltration rate was not measured in this study. It was, however, estimated using empirical equations in Appendix C of ASHRAE Standard 62.2-2016.

Hesaraki and Holmberg (5) implemented an occupant-based ventilation control approach in newly-built Swedish houses, where the ventilation rate was decreased by 27 % during unoccupied periods to save energy. They varied the length of time in which the reduced ventilation was allowed (a range of 4 hours to 10 hours) and estimated what the potential exposure would be to occupants returning home after a prolonged period of reduced ventilation. Their study showed that a heating energy savings of 16 % could be achieved by operating at the reduced ventilation rate for eight hours (and returning to normal ventilation two hours before occupants returned). This study only accounted for mechanical ventilation (i.e., they assumed no infiltration) when determining the concentration of pollutants during the periods of reduced and normal ventilation. Without accounting for infiltration, their estimates of the concentrations of internally-generated contaminants may be elevated.

Turner and Walker (6) simulated potential energy savings of more than 40 % using their Residential Integrated Ventilation Controller (RIVEC), without compromising long-term or short-term exposures to pollutants with constant emission rates. The RIVEC monitored all the ventilation devices in a house, including the kitchen and bathroom exhausts, and reduced mechanical outdoor ventilation when those exhaust systems were running. The RIVEC also took into consideration times of peak electrical demand and times of the day when outdoor pollutants may be high to reduce outdoor ventilation until a more favorable time. Because the mechanical ventilation fan may be switched-off for up to four hours (i.e., during peak electrical demand), the airflow capacity of the installed fan must be 125 % of what is required by ASHRAE Standard 62.2, per the requirements of the standard for intermittent operation [7]. Turner and Walker (6) used the constant ASHRAE Standard 62.2 infiltration credit in their analysis.

A study by Walker and Less (8) used relative dose and exposure for real-time ventilation control using a model developed by Lawrence Berkeley National Laboratory (LBNL) called REGCAP. This is a mass-balance model that accounts for ventilation, heat transfer, equipment operation, and moisture. It was assumed that a generic pollutant is emitted continuously but that occupancy varied throughout the day. Simulations were performed on a single-story home. As in the previous study, the ventilation airflow rate needed to be 2 to 2.5 times higher than the requirement in ASHRAE Standard 62.2-2016 in order to make-up for fan-off times during unoccupied periods. It also needed to be oversized to maintain the annual relative exposure during occupied hours per requirements in the standard for real-time control. Thus, ventilation energy savings were small because the benefits of switching-off ventilation during unoccupied hours was offset by elevated ventilation during occupied hours. Infiltration was calculated in one of two ways: (1) an annual mean effective rate which is constant for the year and (2) using the Alberta Air Infiltration Model (AIM-2) [9, 10]. Relatively small savings in HVAC energy were also reported in Ref. [11] due to the increase in fan operation to make-up for fan-off times. They used CONTAM-EnergyPlus coupled models [12] for their analyses.

Infiltration is dynamic, varying in time by 5-to-1, or more, with ventilation system operation, weather, and indoor conditions [13] Despite this variability, the dynamics are often simplified in ventilation standards and ventilation control strategies. For example, a single infiltration rate is often used even though it may not be appropriate when determining whether the total outdoor air ventilation rate complies with a standard or local code requirements throughout the year. Currently, the most accurate way to determine real-time infiltration rates into a building is through tracer gas testing dilution testing [14]. Infiltration rates determined by tracer gas dilution tests are often averaged over a period of several hours and are only applicable to the weather conditions under which the tests are performed. Tracer gas dilution tests are not currently practical, however, as a means of real-time ventilation control because measurements are taken over a period of several hours and the installation and maintenance of such a system can be costly.

2. Study objective

The objective of this work was to determine how effectively real-time (RT) estimates of infiltration could be used to control residential mechanical ventilation while saving energy and maintaining IAQ according to the standard. The authors propose using airflow simulations to predict RT infiltration rates so that the operation of the mechanical ventilation fan could be reduced or stopped if the RT infiltration is greater than the baseline infiltration credit. Comparisons are made among constant and RT ventilation control strategies in terms of metrics that describe ventilation performance, exposure, and energy use.

3. Infiltration estimation methods

This section describes the infiltration estimation methods used in this study. First, the infiltration credit in ASHRAE Standard 62.2-2016 is described in Section 3.1, and then the CONTAM models used to simulate infiltration for RT control are summarized in Sec. 3.2.

3.1. Infiltration credit

In ASHRAE Standard 62.2-2016 [1], the minimum required outdoor ventilation rate ($Q_{\text{tot,62.2}}$) is determined by:

$$Q_{\text{tot,62.2}}\ (\text{L/s}) = 0.15 \times A_{\text{floor}} + 3.5 \times (N_{\text{br}} + 1) \quad (1)$$

where A_{floor} is the dwelling floor area (m^2) and N_{br} is the number of bedrooms. The standard allows the use of an infiltration credit so that the required rate of mechanical ventilation – which determines the minimum size of the fan and ducts that are installed – can be less than $Q_{\text{tot,62.2}}$. The infiltration credit can be determined in various ways. The normalized leakage (*NL*) method was used in this study:

$$NL = 1000 \times \frac{ELA}{A_{\text{floor}}} \times \left[\frac{H}{H_r}\right]^z \quad (2)$$

where *ELA* is the effective leakage area at 4 Pa measured with a fan pressurization or blower door test (m^2) [15], *H* is the vertical distance between the lowest and highest above-grade points within the dwelling's pressure boundary (m), H_r is the reference height (2.5 m), and z is an exponent to convert *ELA* to an effective annual infiltration rate ($z = 0.4$). All of these parameters are defined in more detail in Standard 62.2. The infiltration credit ($Q_{\text{inf,62.2}}$) is defined as:

$$Q_{\text{inf,62.2}}\ (\text{L/s}) = \frac{NL \times wsf \times A_{\text{floor}}}{1.44} \quad (3)$$

where *wsf* is the weather shielding factor. This factor is based on geographical location (i.e., to capture the climatic conditions) and is assigned as specified in Normative Appendix B of ASHRAE Standard 62.2-2016. Thus, for a single-family detached house,

$$Q_{\text{fan,62.2}}\ (\text{L/s}) = Q_{\text{tot,62.2}} - Q_{\text{inf,62.2}} \quad (4)$$

For cases where a blower door test is not available, ASHRAE Standard 62.2-2016 does not provide a mechanism to estimate *NL*. Despite not being part of the current standard, the authors used two additional methods to estimate *NL*. For one of these methods, air leakage data from 147,000 U. S. houses that comprise LBNL's Residential Diagnostics Database (ResDB) [16, 17] were used. Using these data, LBNL correlated *NL* with the following parameters:

Year of construction (β_{year})
Climate zone (β_{CZ})
House height (m) (β_{h})
Floor area (m^2) (β_{area})

The LBNL approach also accounts for foundation type (β_{floor}) (slab on-grade; unconditioned basement or unvented crawlspace; conditioned basement or vented crawlspace) and location of ductwork (β_{duct}) (conditioned space; unconditioned attic or basement; vented crawlspace). Based on these parameters, *NL* is determined as follows:

$$\ln(NL) = \beta_{year} + \beta_{CZ} + \beta_{area} \cdot \text{Area} + \beta_h \cdot \text{Height} + \beta_{floor} + \beta_{duct} \quad (5)$$

In addition, the LBNL approach allows adjustment of *NL* by Δ*NL* to account for homes that are weatherized or participated in energy efficient programs using the following equation:

$$\Delta NL = -0.128 \cdot NL \cdot -0.000425 \cdot \text{Area} + 0.0146 \cdot \text{Height} \quad (6)$$

For the other method, the kitchen exhaust fans in the test houses (to be described in Sec. 4) were used to conduct a fan depressurization test to estimate the building envelope airtightness and converted to *NL* using Eq. (2). More details on this method will be presented in Sec. 4.2.

3.2. Real-time estimate using CONTAM

Infiltration rates in homes change with time depending on weather, indoor conditions and equipment operation. In this study, real-time infiltration rates are estimated using the multizone airflow simulation software, CONTAM, developed at the National Institute of Standards and Technology (NIST) [18]. CONTAM is particularly useful for whole-building simulation because it fully captures the airflow physics related to building airflow and is computationally efficient. CONTAM also has the advantage in that it can model the impacts of HVAC system operation on infiltration and interzonal airflows. CONTAM has been validated in terms of program integrity [19], and comparisons with laboratory experiments [19] and field studies [19-22].

4. Methods

The objective of this work was to determine how effectively RT estimates of infiltration could be used to control residential mechanical ventilation while saving energy and maintaining IAQ according to the standard. The authors used CONTAM to predict RT infiltration rates in two test houses on the NIST campus and then used those rates to emulate RT mechanical ventilation system controllers. The two test houses, their ventilation requirements, and the measurements of air change rates, pressure differences and other parameters are described in Sec. 4.1. CONTAM models of the test houses are described in Sec. 4.2, starting with detailed models that include every interior zone and closely match the actual floor plans. A method was also developed to create useful, simplified CONTAM models that can be more easily applied in the field. For these simplified CONTAM models, it was assumed that blower door test results would not be available, so the authors evaluated two methods to estimate the building envelope airtightness: (1) the normalized leakage database study described in Sec. 3.1 (the "DB method") and (2) an in-situ fan exhaust depressurization test (the "ExhF method").

Tracer gas decay tests were used to verify the predictive ability of the detailed and simplified CONTAM models (Sec. 4.2 and Sec. 4.3). Sec. 4.4 discusses the four ventilation control strategies that were investigated, including a continuous and three RT control strategies. Sec. 4.5 describes the metrics used to evaluate the performance of the four ventilation control strategies.

4.1. Test houses, ventilation requirements, and measurements

This section describes the two test houses on the NIST campus in Gaithersburg, MD, USA, their ventilation requirements, and the measurements that were conducted in them.

4.1.1.1. IAQ Manufactured House

The IAQ Manufactured House (MH) is a one-story, double-wide, manufactured house built on the NIST campus in 2002 (Fig. 1a). It has three bedrooms, two bathrooms, and an open space containing a living room, dining room, family room, and kitchen. The MH is conditioned with a central, forced-air 22 kW gas furnace and 15 kW electric air conditioner. The supply air distribution ductwork is in an insulated portion of the crawlspace (i.e., belly) that spans the entire floor area of the house (Fig. 1b). Based on prior measurements, air within the supply ducts leaks into the belly [23], such that when the space conditioning system is on, the conditioned areas of the MH are slightly depressurized.

The MH has two bath exhausts, a kitchen exhaust, and a whole-house ventilation exhaust fan. These four exhausts were turned off during the testing. The temperature of the house was measured and the operation of the central heating and cooling system, including its indoor blower, were controlled by a commercially available thermostat. The front and back doors of the attached garage were open during the testing to reduce the garage's impact on the pressure boundary of the house. Table 1 summarizes the characteristics of the MH. Additional details of the MH can be found in Refs. [23, 24].

4.1.1.2. Net-Zero Energy Residential Test Facility

The Net-Zero Energy Residential Test Facility (NZERTF) at NIST was built in 2012 to support the development and adoption of cost-effective net-zero energy designs, technologies, and construction methods (Fig. 2). It is two-story, and has four bedrooms, three bathrooms, and an open living room, dining room, and kitchen space. The NZERTF also has a basement and attic, both located within the conditioned space because the thermal and air-moisture barriers encompass the basement walls and attic roof. Transfer grilles link the living spaces to these two zones. The central heating and cooling system includes an air-to-air heat pump, which delivers air to the basement, first and second floors. The heat pump has a cooling capacity of 7.6 kW and a heating capacity of 7.8 kW. The indoor unit is in the basement and ductwork runs along the basement ceiling. A balanced heat recovery ventilator (HRV) is installed in the basement and has its own dedicated ductwork. The HRV supplies 47 L/s of outdoor air to the house, with supplies on the first floor (in the kitchen/dining area) and in each of the three second-floor bedrooms. Air from the first-floor bathroom and both second-floor bathrooms are exhausted to the HRV before being exhausted. During the testing, the HRV operated on an intermittent schedule (40 min on, 20 min off) to deliver an hourly average of 38 L/s. The house also has a kitchen exhaust and a clothes dryer exhaust, both of which were turned off. The temperature of the house was measured and the operation of the space conditioning system, including its recirculating air distribution fan, were controlled by a commercially available thermostat. Table 1 summarizes the characteristics of the NZERTF. Additional design, construction, equipment, and energy performance details for the NZERTF can be found in Refs. [25-27].

(a)

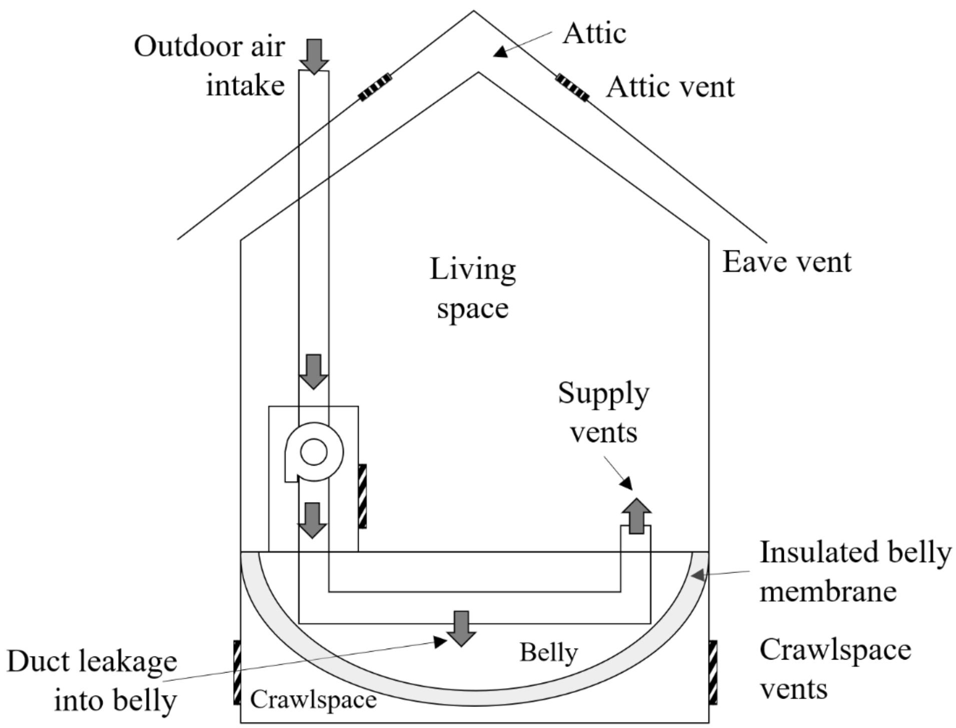

(b)

Fig. 1. (a) Photograph and (b) schematic cross-section of MH showing crawlspace and belly.

Fig. 2. Photograph of NZERTF.

Table 1. Characteristics of MH and NZH.

Building characteristics	**MH**	**NZERTF**
Year of construction	2002	2012
Floor area (m^2)	140	245 (habitable area) 490 (all floors)[a]
Building volume (m^3)	357	1301 (all floors)
Stories	1	3 above ground, includes attic
Height (m)	2.5	6.3
Exterior surface area, above grade (m^2)	301	367
ELA at 4 Pa (cm^2) (from blower door test)	663	137
Heating/Cooling system	22 kW gas furnace 15 kW electric air conditioner	Air-to-air heat pump 7.6 kW cooling capacity 7.8 kW heating capacity
Mechanical ventilation (Design value, L/s)	Components in place, but disabled during this study	HRV, 38[b]

[a]The habitable area of the NZERTF is used to calculate the infiltration credit in ASHRAE Standard 62.2-2016. The total area of the house is used to calculate *NL*.

[b]The mechanical ventilation of 38 L/s is based on ASHRAE Standard 62.2-2010, the standard in effect when the building was designed.

4.1.1.3. Ventilation requirements

The ASHRAE Standard 62.2-2016 requirements for both houses, $Q_{tot,62.2}$, $Q_{inf,62.2}$ and $Q_{fan,62.2}$, are summarized in Table 2 for Atlanta (mixed-humid), Baltimore (mixed-humid), and Chicago (cold). These cities were chosen to represent a range of climatic conditions. Due to its larger size, the NZERTF requires 54 L/s of total outdoor air per ASHRAE Standard 62.2-2016, compared to the MH, which only requires 35 L/s.

Blower door tests were performed on both houses in accordance to ASTM E779-10 [15]. The measured ELA of the MH was 663 $cm^2 \pm 84$ cm^2 and that of the NZERTF was 137 $cm^2 \pm 7$ cm^2. As shown in Table 2, because the NZERTF is tighter than the MH, the $Q_{fan,62.2}$ required (Eq. (4)) at the NZERTF is larger than what is required at the MH. The infiltration credit was determined using Eq. (2) and Eq. (3), where the *wsf* for Atlanta, Baltimore, and Chicago are respectively 0.46, 0.50, and 0.60. Note that ASHRAE Standard 62.2-2016 sets a limit on the infiltration credit so that it cannot exceed 2/3 of $Q_{tot,62.2}$ for new construction (i.e., 36 L/s for the NZERTF and 23 L/s for the MH). For existing homes, Appendix A of ASHRAE Standard 62.2-2016 provides guidance on determining the required mechanical ventilation. For the purposes of this study, it was assumed that both test houses were new construction. Using Eq. (3), the infiltration credit in Chicago for the MH was calculated as 28 L/s, but was set to 23 L/s due to the 2/3's limitation in the standard.

Table 2. ASHRAE Standard 62.2-2016 ventilation requirements and infiltration credit for MH and NZERTF in three cities.

	MH		
Value/City	**Atlanta**	**Baltimore**	**Chicago**
$Q_{tot,62.2}$ (L/s)	35	35	35
$Q_{inf,62.2}$ (L/s)	21	23	23[a]
$Q_{fan,62.2}$ (L/s)	14	12	12
	NZERTF		
Value/City	**Atlanta**	**Baltimore**	**Chicago**
$Q_{tot,62.2}$ (L/s)	54	54	54
$Q_{inf,62.2}$ (L/s)	6	7	8
$Q_{fan,62.2}$ (L/s)	48	47	46

[a]Using Eq. (3), the infiltration credit in Chicago for the MH was calculated as 28 L/s but due to the 2/3s limitation in the standard, its credit is set to 23 L/s.

4.1.1.4. Measurements

Tracer gas decay tests were conducted to measure the whole building air change rate (envelope infiltration plus any mechanical outdoor air intake) in each house under varying conditions, including with the air distribution fans always-on and always-off. Exhaust fans were turned off during the testing. The tracer gas decay tests complied with ASTM E741-11 [14], with sulfur hexafluoride (SF_6) automatically injected at specified time intervals into the return stream of the space conditioning system in the MH and into the HRV supply duct in the NZERTF. In both houses, this injection approach led the tracer gas to be delivered and mixed throughout the house. The tracer gas was sampled in six locations in each house (Fig. 3) at 30 s intervals with a photoacoustic infrared sampler. This instrument has a measurement range of 3.6 mg/m^3 to 18.2 mg/m^3 (0.6 ppm$_v$ to 3 ppm$_v$), and the manufacturer's reported accuracy is 5 % and its rated repeatability is within 1 %.

Differential pressure (ΔP), indoor and outdoor relative humidity (RH), indoor and outdoor temperature (T_{in} and T_{out}, respectively), and wind speed (W_s) were collected during the tests at one-minute intervals (Table 3). At both test houses, T_{in}, T_{out}, and RH (indoor and outdoor) were measured using humidity and temperature probes. ΔP was measured using differential pressure transducers. In the MH, ΔP was measured across each exterior wall and on the wall between the house and open garage at heights of 0.3 m and 1.8 m from the floor (Fig. 3). In the NZH, ΔP was measured across each exterior wall at heights of 0.8 m and 4.3 m from the ground level (i.e., middle of the wall on each floor). W_s was measured at the MH using a sonic anemometer placed 4 m from the south wall and 9 m above the ground. W_s was measured at the NZERTF using an ultrasonic wind sensor located 90 cm above the roof line. The measurement range and accuracy of the sensors are listed in Table 3. Different products were used at the two test houses so that the specifications for measurement range and accuracy in Table 3 are different.

Table 3. Data collected and specifications of instruments.

Data collected	**Measurement range**	**Accuracy**
Differential pressure	± 25 Pa	± 1 % full scale
Indoor dry bulb temperature and relative humidity	MH: -39.2 °C to 60 °C 0.8 % RH to 100 % RH	±0.2 °C ±2 % RH (0 % to 90 % RH) ±3 % RH (90 % to 100 % RH)
	NZERTF: -20 °C to 70 °C 1 % RH to 95 % RH	±0.21 °C (0 °C to 50 °C) ±2.5 % RH (10 % to 90 % RH) ±5 % RH (<10 % and >90 % RH)
Outdoor dry bulb temperature and relative humidity	MH: -39.2 °C to 60 °C 0.8 % RH to 100 % RH	±0.2 °C ±2 % RH (0 % to 90 % RH) ±3 % RH (90 % to 100 % RH)
	NZERTF: -40 °C to 70 °C 0 % RH to 100 % RH	±0.21 °C (0 °C to 50 °C) ±2.5 % RH (10 % to 90 % RH) ±5 % RH (<10 % and >90 % RH)
Outdoor wind speed	MH: 0 m/s to 65 m/s 0 ° to 360 °	± 0.5 m/s or 5 % ± 5 ° at W_s > 2.2 m/s
	NZERTF: 0 m/s to 60 m/s 0 ° to 360 °	± 3 % at 10 m/s ± 3 °

4.2. CONTAM models

Hourly CONTAM simulations were run for each test house using annual Typical Meteorological Year 3 (TMY3) weather files for Atlanta, Baltimore, and Chicago [28]. Two types of CONTAM models were developed for each test house: detailed and simplified. The detailed models were developed using the floor plans and included all rooms in the house. The building envelope airtightness values determined from blower door measurements were also included in the detailed models. The simplified models had single-zone, square floor plans. Two methods for estimating building envelope airtightness for each house were included in the simplified models. For one method, air tightness was estimated using an empirical equation and building characteristics (Sec. 4.2.2.1). A simplified blower door test was used to estimate air tightness for the second method (Sec. 4.2.2.2). Each model is described in more detail first.

4.2.1. Detailed CONTAM models

The detailed CONTAM models (or "CONTAM$_d$" models) of the test houses include every room, including closets and duct shafts in the case of the NZERTF. A detailed description of the MH model, as well as its validation, can be found in Refs. [23, 24]. Validation of a coupled CONTAM-EnergyPlus model of the NZERTF is available in Ref. [29].

In CONTAM, ventilation systems can be modeled either as "simple" or ducted air handling systems (AHS). In the MH, the central heating and cooling system is modeled in CONTAM as a ducted air handling system to capture airflow and contaminant transport between the belly and the habitable areas of the MH. Fig. 4 shows the ductwork at the MH in the belly, which supplies the habitable areas through floor vents. The recirculating fan (labeled as "HVAC fan" on the first floor) is modeled using the Fan Performance fan type in CONTAM, with a cut-off ratio of 0.1, meaning the simulated fan turns off if the calculated airflow is less than 10 % of the maximum airflow. The fan then becomes a simple orifice with an area of 0.02 m^2 to allow airflow through the duct system, to and from the belly, when the fan is off.

Because the HVAC fan affects the depressurization of the MH, it was important to capture its operation in the CONTAM model. This accounting was accomplished by simulating control of a hypothetical heating and cooling system that is uniquely sized based on the local design heating and cooling temperatures (HDT and CDT, respectively), and a chosen indoor setpoint of 23.5 °C, and a representative thermostat deadband of ± 2 °C [30]. HDT and CDT are the temperatures that are exceeded 1 % of the hours in a typical weather year according to Ref. [31]. It was assumed that the system operated two-thirds of the hour when the outside temperature was equal to its HDT or CDT. For temperatures between 23.5 °C and HDT, and between 23.5 °C and CDT, the runtime fraction varied linearly between 0.0 and 0.67. The fan runtime fraction was not allowed to exceed 1.0 at any temperature. Also, the fan runtime fraction was set to 0.0 when the outdoor temperature was between 21.5 °C and 25.5 °C. An example of the controller runtime fraction as a function of outdoor temperature is given in Fig. 5 for Baltimore, MD, USA (HDT = -7.6 °C and CDT = 33.0 °C). The other two U. S. cities included in this study and their respective HDT and CDT were: Atlanta, GA where HDT = -3.0 °C and CDT = 33.1 °C, and Chicago, IL where HDT = -15.3 °C and CDT = 31.4 °C.

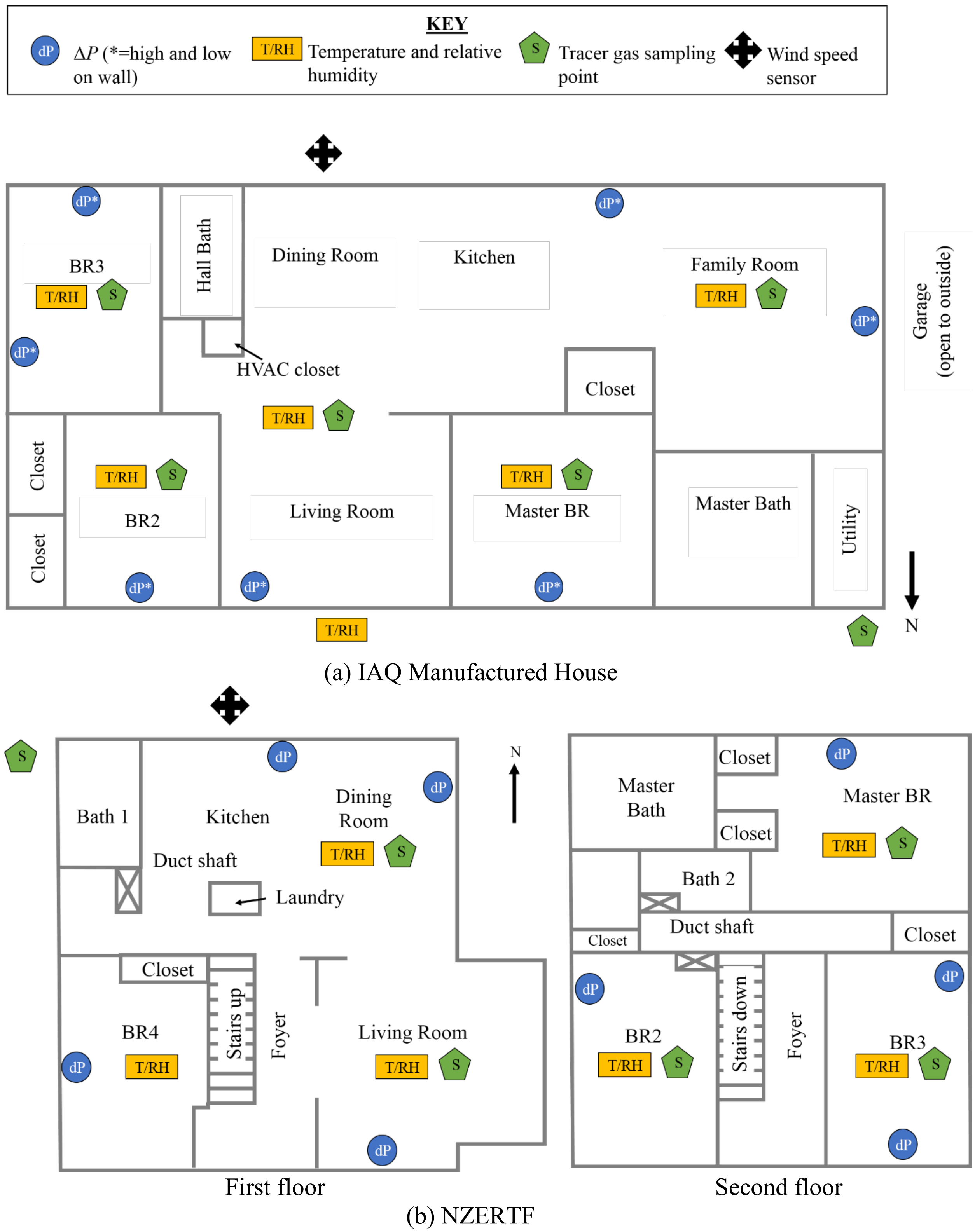

Fig. 3. Location of sensors in (a) MH and (b) NZERTF.

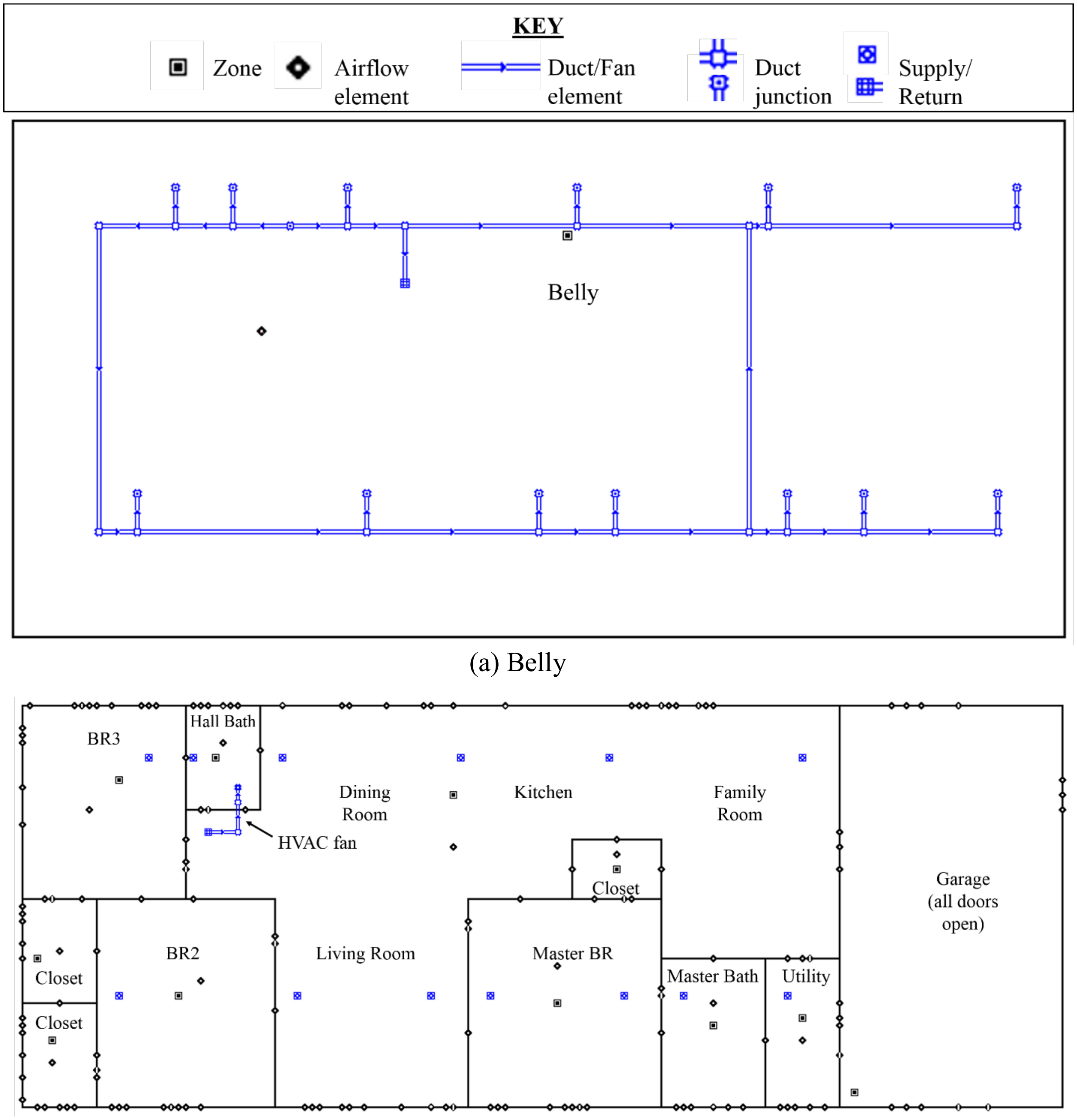

(a) Belly

(b) First floor

Fig. 4. CONTAM model of MH (crawlspace and attic levels not shown).

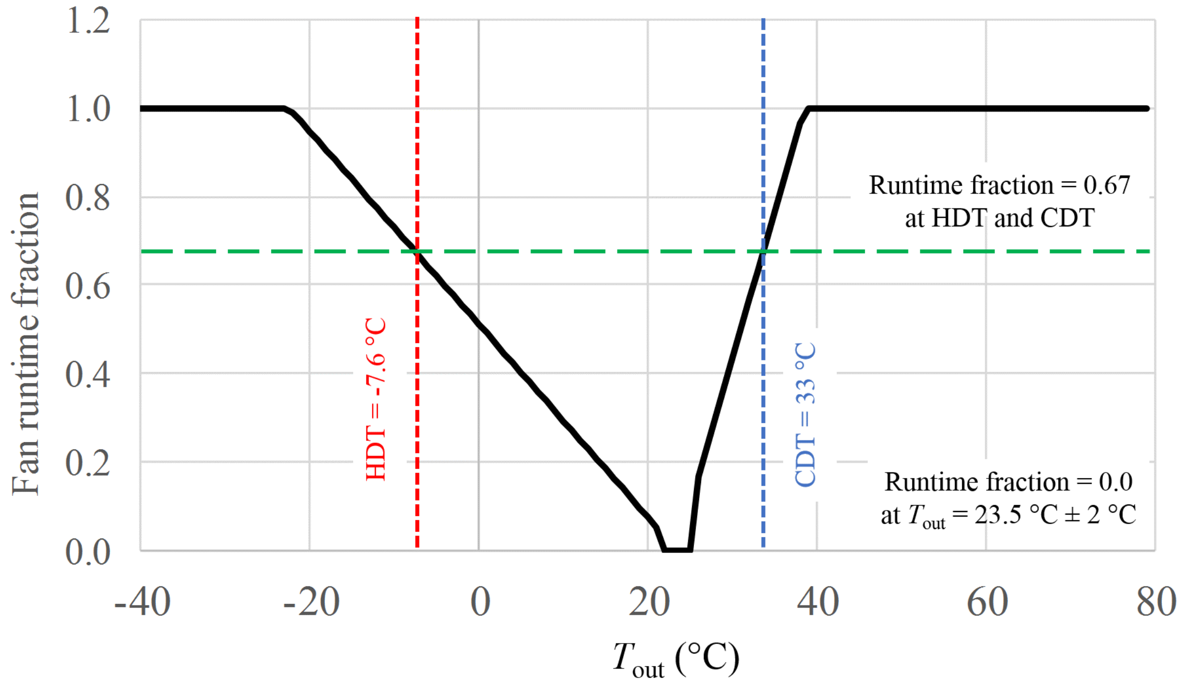

Fig. 5. Simulated fan runtime fraction controller at MH in Baltimore.

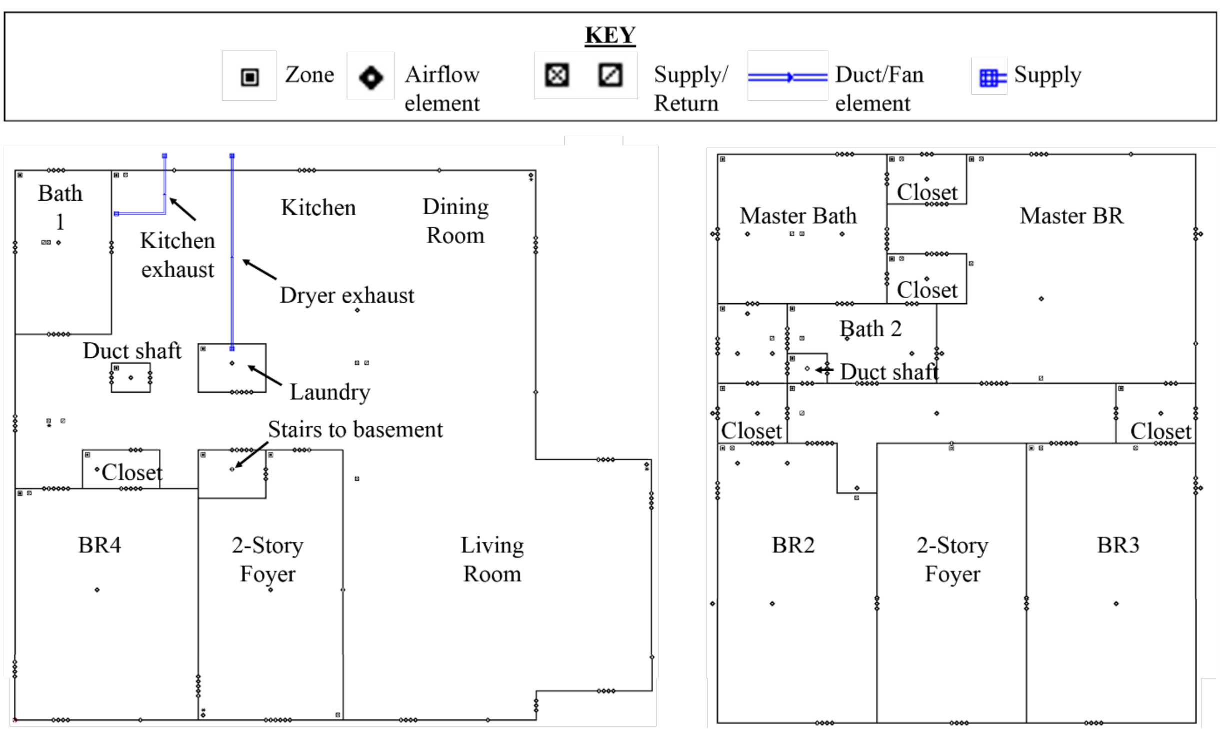

(a) First floor (b) Second floor

Fig. 6. CONTAM model of NZERTF (basement and attic levels not shown).

In the NZERTF, both the heating/cooling and HRV systems are modeled as simple AHS so only supplies and returns are included in the CONTAM model (Fig. 6). The only ductwork included in the CONTAM model of the NZERTF are the kitchen and dryer exhausts on the first floor. The airflow rate at each supply diffuser and return outlet were specified in the model based on airflow rates measured using a low-flow capture hood. Because any duct leakage at the NZERTF is within the conditioned space, fan operation does not impact indoor-outdoor air pressures or infiltration rates. Therefore, a fan runtime controller was not implemented in the CONTAM model, as was done for the MH. Instead, the central heat pump fan was simulated as on continuously. Further, the HRV is a balanced system so its operation does not affect the pressurization of the NZERTF.

There are three leakage sites per section of wall in each model to better capture the stack effect. One leak is placed one-quarter up the height of the wall, another is placed at the middle of the wall, and the third is placed three-quarters up the height of the wall. All the exterior windows and doors were closed and all interior doors were open in the simulations. Results from simulations of the detailed MH and NZERTF models are compared with measurements in Sec. 4.3.

4.2.2. Simplified CONTAM models

The objective of this work was to determine how effectively RT estimates of infiltration could be used to control residential mechanical ventilation while saving energy and maintaining IAQ according to the standard. While CONTAM is not computationally intensive, creating a detailed model of unique houses can be more time-consuming than might be practical for widespread application. Thus, a method was developed to create a simplified CONTAM model (or "CONTAM_s" model). For both houses, the simplified model was one-zone and had a square footprint (Fig. 7). The floor volume is set to the actual house volume and the height of the walls is equal to that of the actual building in Table 1. No ventilation systems were included in the two simplified models. This simplification is more valid for the NZERTF because the heat pump is a recirculating system and the HRV system is balanced. For the MH, however, the simplified model will not capture pressure effects of duct leakage into the belly.

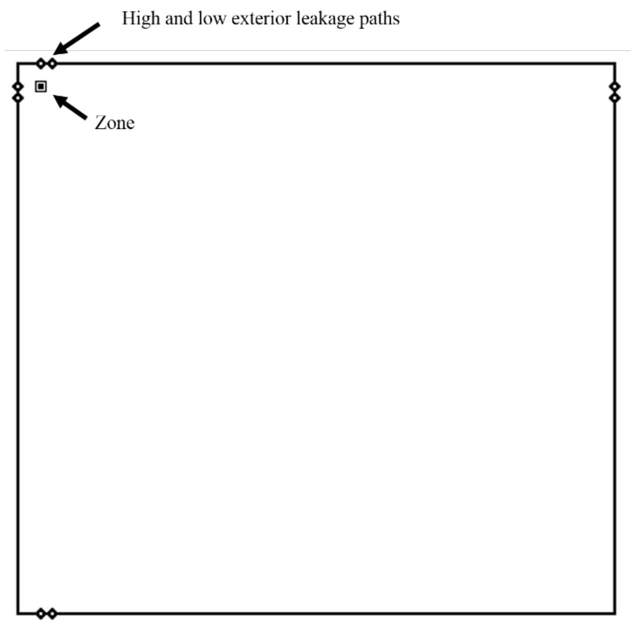

Fig. 7. Simplified CONTAM model.

In anticipation of cases where a blower door test result would not be available, the authors tested two alternative methods of estimating building envelope leakage: (1) the *NL* equation described in Sec. 3.1 (referred to as the "DB" method) and (2) the results of an in-situ fan exhaust test (referred to as the "ExhF" method).

4.2.2.1. DB method

The DB method is based on correlations developed by LBNL that relate measured *NL* data on homes in ResDB with the parameters noted in Section 3.1. As shown in Table 4, even though the MH and NZERTF were built 10 years apart, they were both built after 2000, and their values for β_{year} are the same. For β_h and β_{area}, these values are also the same for the two test houses because the DB method does not breakdown house size into smaller categories. Finally, both NIST test houses are in the same climate zone, so β_{CZ} is also the same. To account for weatherization and energy efficiency improvements in both test houses, Eq. (6) was used to reduce *NL* by ΔNL.

Using Eq (2), *NL* was converted to *ELA* at 4 Pa, and the results were ELA_{MH} = 707 cm^2 and ELA_{NZERTF} = 362 cm^2. These values are compared with the values determined by blower door testing and the ExhF method in Table 5. For use in the CONTAM models, *ELA* was normalized by the exterior surface area of each test house.

To account for the stack effect in the CONTAM$_s$ models, the exterior wall leakage was modeled as two paths on each wall, one at height (h) = 0 m and one at the test house height (H), both with the same normalized leakage value (ELA_{lo} and ELA_{hi}, respectively). The leakage path at h = 0 had a multiplier equal to half the wall exterior surface area. The leakage path at $h = H$ had a multiplier equal to half the wall exterior surface area plus a quarter of the roof exterior surface area. The CONTAM$_s$ model using the DB method for estimating and modeling exterior leakage is referred to as the CONTAM$_{s,DB}$ model.

Table 4. Regression parameters used to determine *NL* and Δ*NL* by DB method.

LBNL regression parameter	MH value	NZERTF value
Year of construction (β_{year})	Built in 2002, β_{year} = -1.058	Built in 2012, β_{year} = -1.058
House height (β_h)	β_h = 0.064	
Climate zone (β_{CZ})	Humid A4, β_{CZ} = 0.326	
Floor area (β_{area})	B_{floor} = -0.00208	
Foundation type	Vented crawlspace, β_{floor2} = 0.18	Conditioned basement, β_{floor1} = 0.109
Duct location	Vented crawlspace, β_{duct2} = 0.181	Conditioned space, β_{slab} = -0.124
Weatherization & energy efficiency improvements	Used Eq. (6) to reduce *NL* by Δ*NL*	

4.2.2.2. ExhF method

For the ExhF method, the kitchen exhaust fans in the MH and NZERTF were used to conduct a fan depressurization test to estimate the building envelope airtightness. In the MH, the kitchen exhaust was operated over four fan speeds with airflow rates between 50 L/s to 200 L/s, resulting in ΔP between -7 Pa and -1 Pa. In the NZERTF, the kitchen exhaust was operated over three fan speeds with airflow rates between 35 L/s to 75 L/s, resulting in ΔP between -10 Pa and -3 Pa. Larger ΔP values were achieved at the NZERTF, even with the lower exhaust flow rates, because of its tighter building envelope.

The ExhF tests at the MH were conducted four times in October 2017. The test conditions varied between ΔT (outdoor-indoor) of -0.6 °C and -8.0 °C, and W_s between 0.9 m/s and 2.6 m/s. Time-series of ΔP at all test locations (with W_s (dots) also on the y-axis) are shown in Fig. 8 for two of the four ExhF tests at the MH. At time (t) = 40 min, the kitchen exhaust fan was switched to Speed 1. At t = 50 min, it was switched to Speed 2, and so on until the kitchen fan was running at its highest speed (Speed = 4) at t = 60 min. In Fig. 8a (10/17/17), the change in ΔP is more apparent than in Fig. 8b (10/26/17) since 10/26/17 was a colder and windier day.

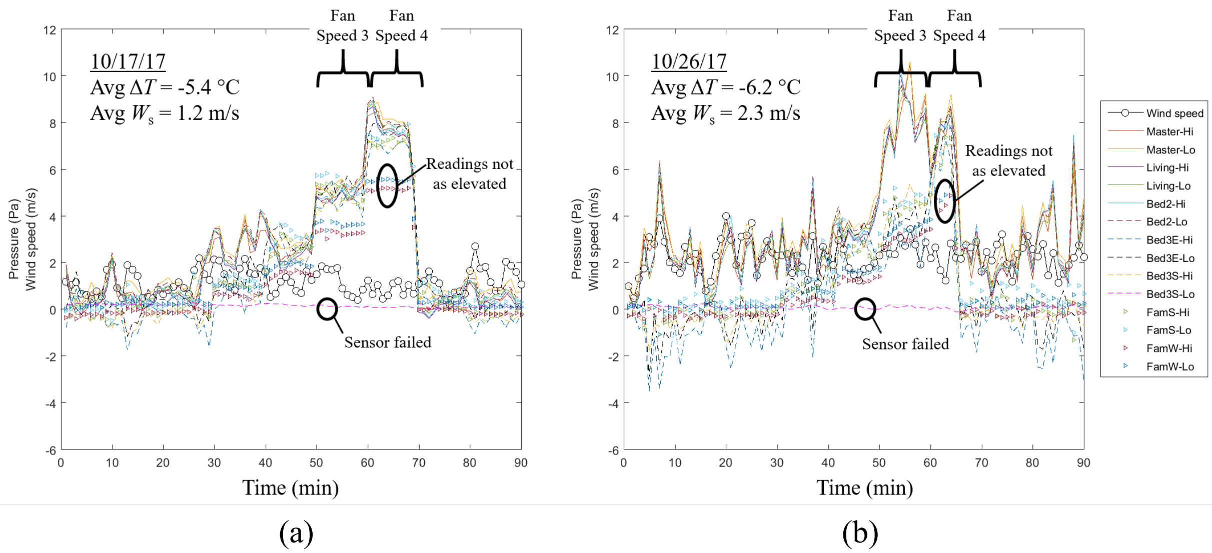

Fig. 8. Plots of ΔP and wind speed vs. time at MH on (a) October 17, 2017 and (b) October 26, 2017.

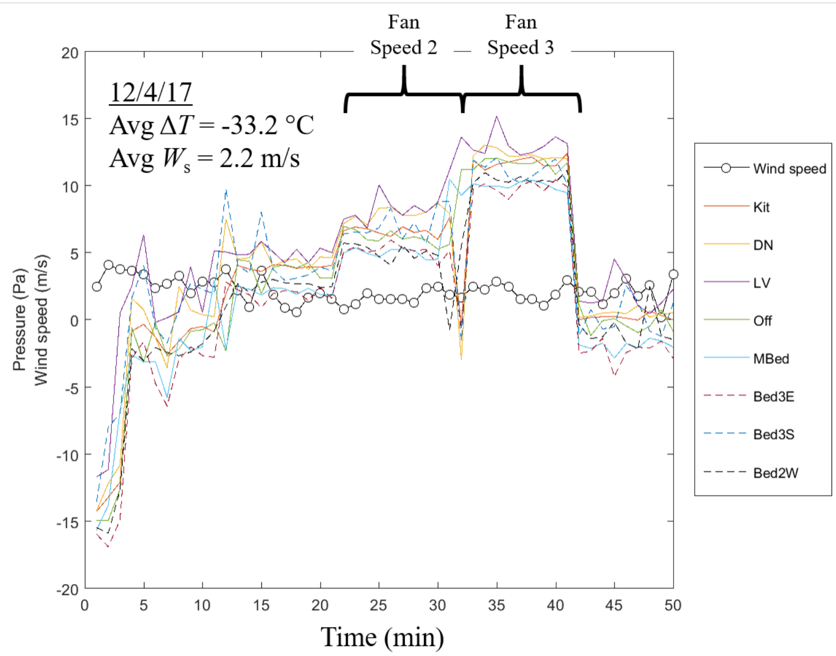

Fig. 9. Plots of ΔP and wind speed vs. time at NZERTF on December 4, 2017.

Measurements from three sensors were not included in the calculation of average ΔP of the test. One ΔP sensor failed (pink dotted line, Bed3S-Lo) during the test. Two sets of ΔP measurements followed similar trends as the other measurements but were not as elevated as the others. These sensors were in the Family Room, on the west wall (pink and blue triangles, FamW-Hi and FamW-Lo), which is adjacent to the garage. Even though the garage doors were fully open during the entire duration of this study, the ΔP measurements at the house-garage interface were excluded from the analysis. Due to time constraints at the NZERTF, only one ExhF test was conducted on December 4, 2017. Fig. 9 shows an apparent change in ΔP at t = 20 min and t = 30 min when the kitchen exhaust fan was at its two highest settings (Speed = 2 and Speed = 3).

Following the procedure in ASTM E779-10 for depressurization tests [15], the *ELA* at 4 Pa from the ExhF tests are summarized in Table 5. These values are compared with both the *ELA* at 4 Pa value from the DB method and with the results from the blower door tests conducted by NIST. The CONTAM_s model using the ExhF method for estimating and modeling exterior leakage is referred to as the $\text{CONTAM}_{s,E}$ model.

Table 5. Summary of *ELA* at 4 Pa values for NIST test houses determined by various methods.

NIST test house	Blower Door	Database (DB)	Exhaust Fan (ExhF)
MH	663 cm^2 ± 84 cm^2	707 cm^2	580 cm^2 ± 280 cm^2
NZERTF	137 cm^2 ± 7 cm^2	362 cm^2	152 cm^2 ± 15 cm^2

To account for the stack effect, the approach for modeling exterior wall leakage for the $\text{CONTAM}_{s,E}$ model was modified from the approach used for the $\text{CONTAM}_{s,DB}$ model. Again, two leakage paths are modeled on each wall, at h = 0 m (multiplier equal to half the wall area) and at the $h = H$ m (multiplier equal to half the wall exterior surface area plus a quarter of the roof exterior surface area). Instead of the leakage values being equal, as they were for the $\text{CONTAM}_{s,DB}$ model, the leakage values for the $\text{CONTAM}_{s,E}$ model were different for the two leaks. Their difference depended on the location of the neutral pressure level (NPL), and so better accounts for the vertical distribution of the envelope air leakage. Neglecting differences in the density of air, the NPL can be determined using Ref. [32]:

$$\text{NPL} = \frac{H}{1+\left(\frac{ELA_{\text{lo,f}}}{ELA_{\text{hi,f}}}\right)^{\frac{1}{n}}} \tag{7}$$

where $ELA_{\text{lo,f}}$ and $ELA_{\text{hi,f}}$ are respectively the fraction of the exterior leakage that is attributed to the lower and upper portions of the building and n is the flow exponent (n = 0.65). The sum of $ELA_{\text{lo,f}}$ and $ELA_{\text{hi,f}}$ must equal 1.0. Differential pressure measurements were taken at both test houses when the systems were off to estimate NPL. Using only the data when wind speed was less than 2 m/s, three test periods at the MH and one test period at the NZERTF were available. Using the sensor heights of 0.3 m and 1.8 m at the MH, 0.8 m and 4.3 m at the NZERTF, a slope and intercept were calculated and used to determine the NPL (i.e., at ΔP = 0) (Table 6).

Using Eq (7), $ELA_{\text{hi,f}}$ was varied (and $ELA_{\text{lo,f}}$ set equal to 1 - $ELA_{\text{hi,f}}$) until the calculated NPL was equal to NPL_{avg} determined using ΔP measurements. The calculated $ELA_{\text{lo,f}}$ and $ELA_{\text{hi,f}}$ confirmed that the MH has a leaky roof ($ELA_{\text{lo,f}} < ELA_{\text{hi,f}}$) and that the NZERTF has a tight roof ($ELA_{\text{lo,f}} > ELA_{\text{hi,f}}$).

Table 6. Measurements and calculated values used to determine exterior leakage distribution.

	MH			NZERTF
	Test period 1	**Test period 2**	**Test period 3**	**Test period 1**
Avg W_s (m/s)	1.5	1.7	0.6	1.3
Avg ΔT (°C)	-6.5	-7.6	-6.8	-30.7
ΔP_{lo}	-1.5	-1.6	-0.9	-1.4
ΔP_{hi}	-0.5	-0.2	-0.1	3.4
Slope ($\Delta P/h$)	0.7	0.9	0.6	1.4
Intercept (ΔP)	-1.7	-1.9	-1.1	-2.4
NPL (m)	2.5	2.0	1.9	1.8
NPL_{avg} (m)		2.2		1.8
$ELA_{lo,f}$		0.23		0.65
$ELA_{hi,f}$		0.77		0.35
ELA_{lo} (cm²/m²)		0.4		0.2
ELA_{hi} (cm²/m²)		1.5		0.1

The NPL_{avg} of the MH (2.2 m) is nearly as high as its height of 2.5 m. The NPL_{avg} of the NZERTF (1.8 m) is less than half its height of 6.3 m. Thus, for the $CONTAM_{s,E}$ model, the distribution of roof-to-wall leakage in the MH was 0.77/0.23, meaning that 77 % of the exterior envelope leakage was modeled at $h = H$ m and 23 % was modeled at $h = 0$ m. At the NZERTF, the distribution of roof-to-wall leakage was 0.35/0.65. These fractions were then multiplied by the *ELA* (ExhF methods only) in Table 5 to obtain ELA_{lo} and ELA_{hi} for each test house (Table 6).

4.3. CONTAM verification tests

Tracer gas decay measurements of whole building air change rates were used to verify the detailed CONTAM models of the test houses. In turn, rates predicted by the simplified CONTAM models were then compared with those predicted using the detailed CONTAM models. Fourteen decay tests were performed in the MH in October 2017 (8 with the system heating/cooling system on, 6 with the heating/cooling system off). At the NZERTF, eight tests were performed in December 2017 (6 with the heating/cooling system and HRV on, 2 with the heating/cooling system and HRV off). The outdoor air change was calculated using the procedure in ASTM E741-11 [14]. Table 7 and Table 8 show the average temperature difference (T_{out}-T_{in}) and wind speed (W_s) during the tests. On average, the tests at the MH were conducted in milder weather than the tests conducted at the NZERTF [14].

Table 7 shows the measured and predicted air change rates for the MH, where the average measured total outdoor airflow rate (mechanical ventilation plus infiltration) with the heating/cooling system on was 21 L/s with a 95 % confidence interval of ± 0.2 L/s (Table 7). The average predicted rate was 18 L/s (average absolute difference of 14 %). With the heating/cooling system off, the measured total outdoor airflow rate was 18 L/s with a 95 % confidence interval of ± 0.2 L/s, and the average predicted rate was 16 L/s (average absolute difference of 22 %). As noted earlier, the mechanical ventilation system in the MH was off, so the space conditioning system on and off air change rates were expected to be similar, except for the additional infiltration and duct leakage into the belly.

Table 8 shows the measured and predicted air change rates for the NZERTF. The average measured total outdoor airflow rate with the system on was 60 L/s with a 95 % confidence interval of ±2 L/s, and the average predicted rate was 52 L/s (average absolute difference of 12 %). Both the measured and predicted rates included the outdoor mechanical ventilation provided by the HRV. There was one 4-hr period during Test #4, and one 2-hr period during Test #6, when the HRV recirculation mode was activated because the outside temperature was below -10 ° C. The average measured total outdoor airflow rate with the system off was 22 L/s ± with a 95 % confidence interval of 0.5 L/s, and the average predicted rate was 18 L/s (average absolute difference of 18 %).

In summary, the absolute differences between the measured and predicted rates ranged between 4 L/s and 7 L/s at the MH, and between 1 L/s and 18 L/s at the NZERTF, including both the system-on and system-off values. These differences were on average 15 % of the average measured outdoor airflow rate at each test house. These rates translate to an average of 0.05 h^{-1} difference at the MH, and 0.03 h^{-1} difference at the NZERTF. As noted in Ref. [33], at rates this low, the measurement accuracy of the tracer gas decay measurements needs to be considered. Further, ASTM E741-11 [14] states that following its procedure, measurements of gas concentrations will provide air change rate values within 10 % of the true value. Given the low air change rates and stated uncertainty in ASTM E741-11, the results of the CONTAM_{d} models were considered to be within reasonable accuracy. Comparisons of measured and predicted infiltration rates have also yielded differences with similar magnitude [34-36]. Thus the CONTAM_{d} models were used to compare the results of the CONTAM_{s} models and their impact on RT ventilation control.

4.4. Ventilation control strategies

As noted earlier, this study involved the evaluation of four ventilation control strategies, including one continuous and three RT control strategies. The four ventilation strategies considered were:

1. $\underline{\text{Vent}_{\text{cont}}}$: This strategy continuously supplied each test house with $Q_{\text{fan,62.2}}$ as defined by Eq. (4). The hourly infiltration rates for this strategy are predicted by the detailed CONTAM model, CONTAM_{d}.
2. $\underline{\text{Vent}_{\text{RT-d}}}$: This strategy implemented RT ventilation control by supplying each test house with $Q_{\text{fan,RT-d}}$ that varied with each timestep depending on the infiltration rate calculated by CONTAM_{d}, such that $Q_{\text{fan,RT-d}} = Q_{\text{tot,62.2}} - Q_{\text{inf,d}}$. As discussed below, if $Q_{\text{inf,d}} > Q_{\text{tot,62.2}}$, then $Q_{\text{fan,RT-d}} = 0$. (This same restriction is placed on the $\text{Vent}_{\text{RT-DB}}$ and $\text{Vent}_{\text{RT-E}}$ strategies described below.)
3. $\underline{\text{Vent}_{\text{RT-DB}}}$: This strategy implemented RT ventilation control by supplying each test house with $Q_{\text{fan,RT-DB}}$ that varied with each timestep depending on the infiltration rate calculated by $\text{CONTAM}_{\text{s,DB}}$ (the simplified model using the leakage value from the DB method,) such that $Q_{\text{fan,RT-DB}} = Q_{\text{tot,62.2}} - Q_{\text{inf,DB}}$.
4. $\underline{\text{Vent}_{\text{RT-E}}}$: This strategy implemented RT ventilation control by supplying each test house with $Q_{\text{fan,RT-E}}$ that varied with each timestep depending on the infiltration rate calculated by $\text{CONTAM}_{\text{s,E}}$ (the simplified model using the leakage value from the ExhF method) such that $Q_{\text{fan,RT-E}} = Q_{\text{tot,62.2}} - Q_{\text{inf,E}}$.

Two fan-sizing scenarios were considered in evaluating the RT control strategies (Fig. 10). In the first (Scenario 1), the $Q_{fan,RT}$ values are allowed to be greater than $Q_{fan,62.2}$ in order to achieve $Q_{tot,62.2}$ when the predicted RT infiltration is less than the $Q_{inf,62.2}$. In Scenario 2, the $Q_{fan,RT}$ values are limited to $Q_{fan,62.2}$. It was assumed that $Q_{fan,RT}$ could be achieved by scheduling the fan to operate a fraction of the hour that is equal to the ratio of $Q_{fan,RT}$ to the maximum flow rate (e.g., $Q_{tot,62.2}$ for Scenario 1).

For the Vent $_{RT\text{-}d}$, Vent $_{RT\text{-}DB}$, and Vent $_{RT\text{-}E}$ control strategies, $Q_{fan,RT}$ is determined by subtracting the predicted Q_{inf} (from the respective CONTAM models) from $Q_{tot,62.2}$. As Fig. 10 shows, if $Q_{inf} > Q_{tot,62.2}$, then $Q_{fan,RT} = 0$. For Scenario 1, there is no upper limit on $Q_{fan,RT}$ so that the total outdoor ventilation ($Q_{inf} + Q_{fan,RT}$) could be greater than $Q_{tot,62.2}$. Further, the maximum airflow rate of the fan is equal to $Q_{tot,62.2}$, so that the outdoor ventilation requirement is met even when infiltration is close to zero. In Scenario 2, Q_{fan} cannot exceed $Q_{fan,62.2}$ so that $Q_{tot,62.2}$ may not always be met. For the Vent$_{cont}$ strategy, Q_{fan} is equal to $Q_{fan,62.2}$ and does not vary.

Table 7. Measured and predicted $CONTAM_d$ total outdoor airflow rates for MH.

System status	Test number	Average T_{out}-T_{in} (°C)	Average W_s (m/s)	Measured total outdoor airflow rate (L/s)	95 % confidence interval of measured value (L/s)	Predicted total outdoor airflow rate (L/s)	Percentage difference (%)
On	1	3	1	21	0.3	14	33
On	2	-7	1	15	0.1	15	0
On	3	4	4	30	0.2	25	17
On	4	-1	3	23	0.2	21	9
On	5	1	1	17	0.2	13	24
On	6	-2	4	24	0.1	23	4
On	7	4	2	23	0.3	19	17
On	8	-5	0	12	0.1	13	-8
On	**Average tests 1 to 8**	**0**	**2**	**21**	**0.2**	**18**	**14**
Off	9	-2	1	9	0.1	8	11
Off	10	-3	3	14	0.1	18	-29
Off	11	-6	4	19	0.4	22	-16
Off	12	-7	2	23	0.2	18	22
Off	13	-8	2	21	0.2	17	19
Off	14	-7	1	20	0.1	15	25
Off	**Average tests 9 to 14**	**-5**	**2**	**18**	**0.2**	**16**	**20**

Table 8. Measured and predicted $CONTAM_d$ total outdoor airflow rates for NZERTF.

System status	Test number	Average T_{out}-T_{in} (°C)	Average W_s (m/s)	Measured total outdoor airflow rate (L/s)	95 % confidence interval of measured value (L/s)	Predicted total outdoor airflow rate (L/s)	Percentage difference (%)
On	1	-21	3	77	3	59	23
On	2	-22	2	68	3	54	21
On	3	-24	4	66	3	59	11
On	4	-31	5	42[a]	2	41	2
On	5	-28	3	63	2	58	8
On	6	-30	1	43[a]	1	40	7
On	**Average of tests 1 to 6**	**-26**	**3**	**60**	**2**	**52**	**12**
Off	7	-25	2	17	0.3	18	-6
Off	8	-31	1	27	0.4	19	30
Off	**Average of tests 7 and 8**	**-28**	**2**	**22**	**0.5**	**18**	**18**

[a]The HRV was in recirculation mode during part of these tests to prevent frosting of the heat exchanger.

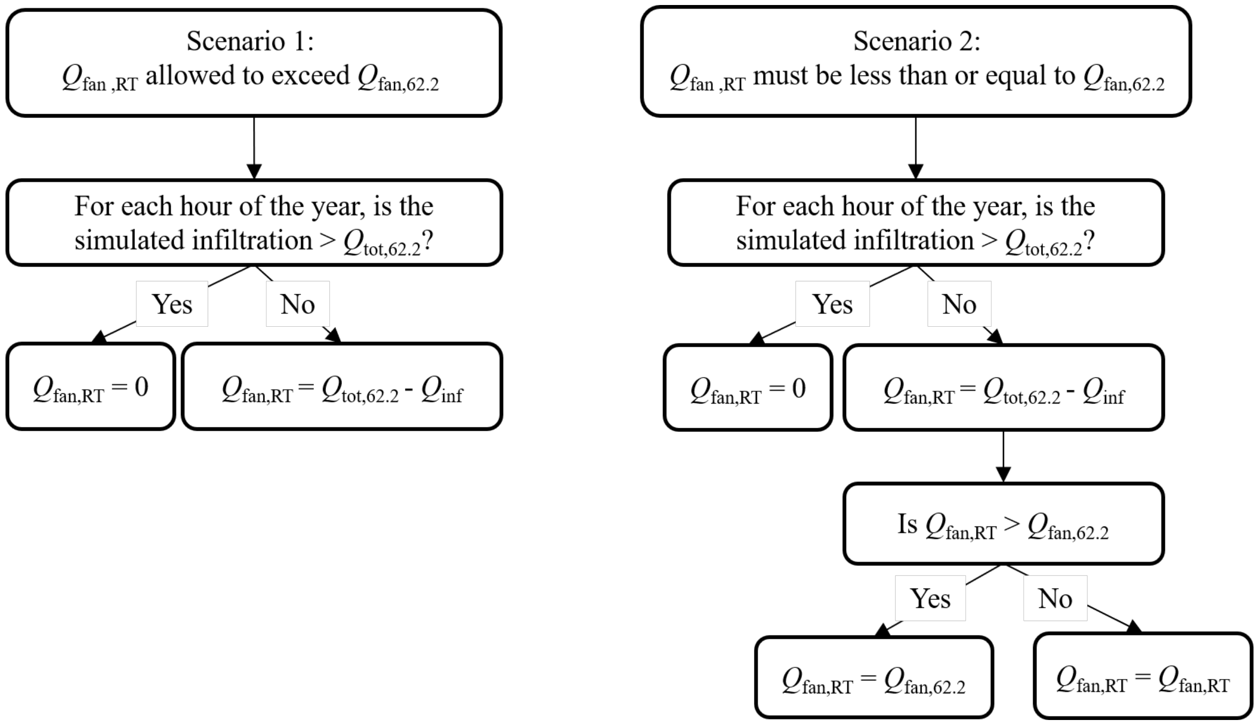

Fig. 10. Flow chart showing how $Q_{fan,RT}$ is calculated at every hour for Scenarios 1 and 2.

4.5. Performance metrics for comparing ventilation control strategies

To compare the performance of the four ventilation control strategies, the following five metrics were used: predicted infiltration rates, average Q_{fan} flow rate, ventilation hours, relative exposure factor, and energy impacts of ventilation.

4.5.1. Predicted infiltration rates

The annual average predicted infiltration rate for the two test houses in three cities is compared among the three CONTAM models. They are also compared with the infiltration credit in ASHRAE 62.2-2016.

4.5.2. Average Q_{fan} flow rate

For the RT ventilation control strategies ($Vent_{RT-d}$, $Vent_{RT-DB}$, $Vent_{RT-E}$), the infiltration rate predicted by each of the respective CONTAM models was subtracted from the total ventilation requirement using Eq. (4) to obtain $Q_{fan,RT}$ at every hour of the year. The annual average $Q_{fan,RT}$, which include the times when the fan was off (i.e., $Q_{fan,RT} = 0$), was calculated for each case. These values are compared with $Q_{fan,62.2}$.

4.5.3. Ventilation hours

At each hourly timestep, whether and how $Q_{tot,62.2}$ was met was evaluated. Outdoor air ventilation was either met by infiltration-alone or by the sum of $Q_{fan,RT}$ and Q_{inf}. Any timesteps where the sum of Q_{fan} and Q_{inf} was less than $Q_{tot,62.2}$ were considered an unmet ventilation hours.

4.5.4. Relative exposure factor

ASHRAE Standard 62.2-2016 allows RT ventilation control only if the annual average relative exposure factor (R_{avg}) during occupied periods does not exceed 1.0 when compared with the exposure that would result from ventilating continuously at $Q_{tot,62.2}$. Further, the relative exposure at any time step (R_i) must not be greater than 5.0 for time steps not to exceed one hour. Based on ASHRAE Standard 62.2-2016 Normative Appendix C, and assuming a generic constant contaminant source that is spatially uniform, R_i is:

$$R_i = {Q_{\text{tot},62.2}}/{Q_{\text{tot},i}} + \left(R_{i-1} - {Q_{\text{tot},62.2}}/{Q_{\text{tot},i}}\right) \times e^{-Q_{\text{tot},i}/V} \tag{8}$$

where i is the ith timestep, and V is conditioned volume (m^3) of the home. In this study, relative exposure at every hour of the year was evaluated. Normative Appendix C to Standard 62.2 provides several methods for determining Q_{inf}, including converting NL from Eq. (2) to a constant infiltration rate using Eq. (3). The user may also calculate the stack- and wind-driven flows using empirical equations for every time step, given the weather and T_{in} at every time step, for an infiltration rate at every timestep. The standard states that these infiltration estimation methods can only be used if a blower door test has been performed. Otherwise, Q_{inf} is set to zero. However, the first of these methods for determining Q_{inf} (using NL with Eq. (3)) assumes that infiltration is constant throughout the year. The empirical equations used in the second method vary infiltration with weather but may not fully capture wind effects on infiltration because the wind coefficients used are averaged over the entire building and not dependent on the specific wind direction. In this study, infiltration is predicted using detailed and simplified CONTAM models for the specific buildings being studied, which more accurately accounts for variations in indoor and outdoor conditions. Note that in Eq. (8), the occupant exposure is relative to the total ventilation rate required by ASHRAE Standard 62.2-2016.

4.5.5. Energy impacts of ventilation

The energy impact of ventilation was evaluated in this study in terms of: (1) the energy to operate the mechanical ventilation (MV) fan (2) the energy to condition the MV air, and (3) the energy to condition the infiltration air. The energy required was then converted to energy cost using an assumed cost of electricity per kilowatt-hour (kWh). Hourly values of the energy to operate the MV fan, E_{MV}, were calculated using Eq. (9), assuming a ventilation fan efficiency (e_{MV}) of 0.5 L/(s•W). This is the average efficiency of HRVs in the Heating Ventilating Institute (HVI) equipment database for fans with the capacity to supply $Q_{tot,62.2}$ in both houses [37].

$$E_{\text{MV}}[\text{kWh}] = {Q_{\text{fan}}}/{e_{\text{MV}}} \times \frac{1}{1000} \times 1\ \text{hr} \tag{9}$$

where Q_{fan} is the hourly fan airflow rate and 1/1000 is a conversion factor from W to kW.

Hourly values of the energy required to condition the MV and infiltration air were determined by calculating the sensible heat of the air being delivered to the test house at T_{out} and conditioned to the indoor setpoint (T_{in}) of 23.5 °C. The effects of latent heat and heat recovery on the heating/cooling load of the test houses was not considered in this study. The sensible heat associated with the MV air, $q_{sens,MV}$, is thus:

$$q_{\text{sens,MV}}[\text{kWh}] = Q_{\text{fan}} \times 3.6 \times \rho \times c_{p,\text{air}} \times (T_{\text{in}} - T_{\text{out}}) \times \frac{1}{3600} \times 1\ \text{hr} \tag{10}$$

where $c_{p,air}$ is the specific heat of air (1.003 kJ/kg• °C), ρ is the density of air (1.2 kg/m^3), 3.6 is a conversion factor from L/s to m^3/s, and 1/3600 is a conversion factor from hour to second. The sensible heat of the infiltration air is calculated the same way, replacing $q_{sens,MV}$ with $q_{sens,inf}$ and replacing Q_{fan} with Q_{inf} in Eq (10).

As a reminder, the MH is conditioned by an electric air-conditioner and heated by a gas furnace. The NZERTF is heated and cooled by an air-to-air heat pump. For simplicity in comparing the energy impacts in the two test houses, it was assumed that the heating/cooling systems in both test houses were both heat pumps with the same performance. The hourly energy required for the heat pump to condition the outdoor air (MV and infiltration air) ($E_{hp,MV}$ and $E_{hp,inf}$) was calculated assuming a heat pump (hp) coefficient of performance (COP) of 3.6 kW/kW. This value is the average COP of heat pumps in the Air-Conditioning, Heating and Refrigeration Institute (AHRI) database with heating and cooling capacities between 7.3 kW and 15 kW, which covers the capacities of the equipment in the test houses [38]. The energy required by the heat pump to condition MV and infiltration air was thus expressed as:

$$E_{hp,MV}[\mathrm{kWh}] = {q_{sens,MV}}/{\mathrm{COP}} \times 1\ \mathrm{hr} \tag{11}$$

$$E_{hp,inf}[\mathrm{kWh}] = {q_{sens,inf}}/{\mathrm{COP}} \times 1\ \mathrm{hr} \tag{12}$$

The hourly cost to operate the MV fan and condition the outdoor air were calculated by multiplying the energy use (kWh) by the national average cost of electricity for 2018-2019 as determined by the U. S. Energy Information Administration. This average value is \$0.13/kWh [39]. The energy savings predicted for each of the RT ventilation control strategies was compared with the $\mathrm{Vent_{cont}}$ strategy.

5. Results

Analyses of the four ventilation control strategies include comparisons of five performance metrics described in Sec. 4.5, which are predicted infiltration rates (Sec. 5.1), average Q_{fan} flow rate (Sec. 5.2), ventilation hours (Sec. 5.3), relative exposure factor (Sec. 5.4) and energy impacts of ventilation (Sec. 5.5).

5.1. Predicted infiltration rates

Table 9 and Table 10 show the average predicted infiltration rate for the detailed and the two simplified CONTAM models, as well as the ASHRAE Standard 62.2-2016 infiltration credit ($Q_{inf,62.2}$) for each test house and city studied.

Table 9 shows that for the MH, the annual average infiltration rate is similar among the three CONTAM models ($\mathrm{CONTAM_d}$, $\mathrm{CONTAM_{s,DB}}$, and $\mathrm{CONTAM_{s,E}}$), and that the predicted annual infiltration rate was greater than the ASHRAE Standard 62.2-2016 infiltration credit. The largest difference between the predicted infiltration rate and $Q_{inf,62.2}$ was in Chicago, where $\mathrm{CONTAM_d}$ estimated an average infiltration rate that is a little more than double $Q_{inf,62.2}$. Table 9 also shows the standard deviation in the annual infiltration rates, which are relatively large with regards to the average value. This indicates that infiltration varies greatly throughout the year, which the ASHRAE Standard 62.2-2016 infiltration credit does not capture.

Table 9. Predicted annual average infiltration rates (± standard deviation) and infiltration credit for MH

Annual average infiltration rate (L/s)	Atlanta	Baltimore	Chicago
Simulation: $Q_{inf,d}$	33±20	37±22	47±26
Simulation: $Q_{inf,DB}$	32±20	33±22	39±23
Simulation: $Q_{inf,E}$	34±21	34±23	41±25
Infiltration credit: $Q_{inf,62.2}$	21	23	23[a]

a. As noted also in Sec. 4.1, the infiltration credit in Chicago for the MH was calculated as 28 L/s but due to the 2/3s limitation in the standard, its credit is set to 23 L/s.

Most of the difference between the predicted infiltration and infiltration credit in Chicago can be attributed to the heating months as seen in Fig. 11. This figure shows the monthly average infiltration rate predicted by each CONTAM model, as well as the infiltration credit ($Q_{inf,62.2}$) and total ventilation rate required by ASHRAE Standard 62.2-2016 ($Q_{tot,62.2}$) for the MH in Chicago. For the bulk of heating months (October to March), the infiltration credit for the MH underestimates the infiltration rate by between 93 % and 135 % (average 110 %) depending on the CONTAM model. In cooling months, the infiltration credit also underestimates the infiltration rate, but only by between 43 % and 68 % (average 53 %). Graphs of monthly average infiltration rates for Atlanta and Baltimore show similar trends and are not presented. It should also be noted that in the heating months, the predicted infiltration alone could on average meet $Q_{tot,62.2}$ at the MH for all three cities.

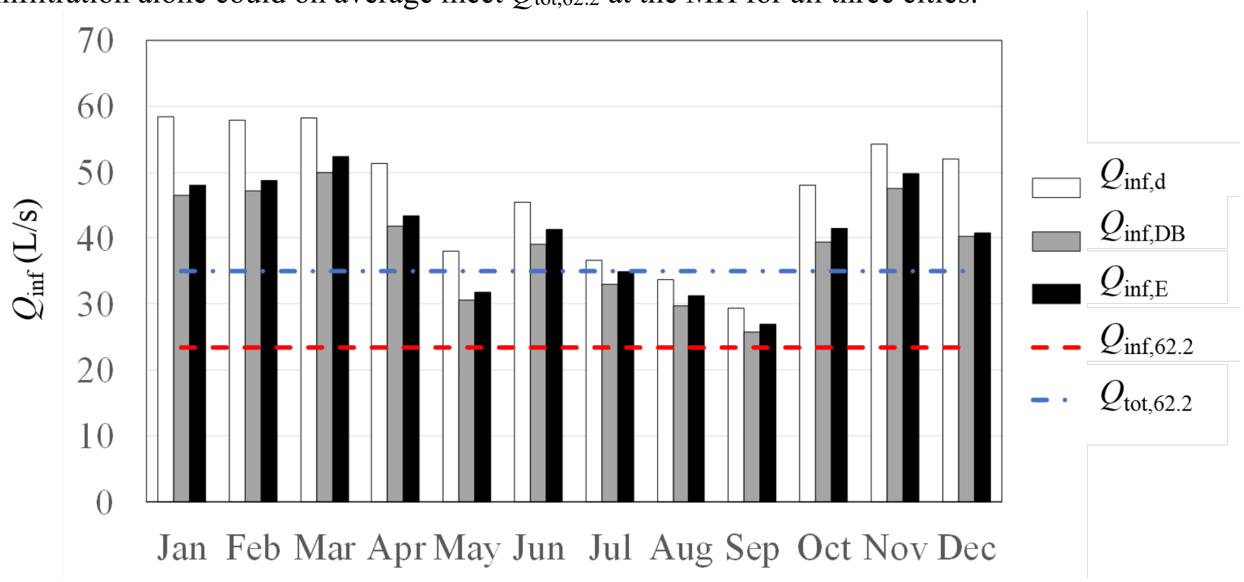

Fig. 11. Monthly average infiltration predicted by three CONTAM models in Chicago at the MH. The horizontal lines show the infiltration credit and total outdoor airflow rate required by ASHRAE Standard 62.2-2016.

Table 10 shows that for the NZERTF, the annual infiltration rates vary more among the three CONTAM models than they did in the MH. This result is not surprising given that the range of *ELA* values across the three CONTAM models at the MH was 18 % compared with a range of 62 % for the NZERTF. For the NZERTF, the CONTAM$_{s,DB}$ model predicted the highest infiltration rate, as it had the largest *ELA*. The NZERTF CONTAM$_d$ model predicted on average 24 % less infiltration, and the CONTAM$_{s,E}$ model predicted on average 61 % less infiltration, relative to the CONTAM$_{s,DB}$ model. Even though the annual average infiltration predicted by the CONTAM$_{s,E}$ model (8 L/s to 10 L/s for the three cities) is very similar to the ASHRAE Standard 62.2-2016 infiltration credit (6 L/s to 8 L/s), the CONTAM$_{s,E}$ model predicts infiltration rates with a standard deviation of 6 L/s (Table 10).

Table 10. Predicted annual average infiltration rates (± standard deviation) and infiltration credit for NZERTF.

Annual infiltration rate (L/s)	Atlanta	Baltimore	Chicago
Simulation: $Q_{inf,d}$	16±10	18±11	21±11
Simulation: $Q_{inf,DB}$	22±13	23±14	27±15
Simulation: $Q_{inf,E}$	8±5	9±5	10±6
Infiltration credit: $Q_{inf,62.2}$	6	7	8

Table 10 shows that at the NZERTF, for all three cities, $Q_{inf,d}$ is on average 2.5 times more than $Q_{inf,62.2}$. Most of the difference can be attributed to the heating months, as shown in Fig. 12 for Chicago. Fig. 12 shows the monthly average infiltration rate predicted by each CONTAM model, as well as the infiltration credit ($Q_{inf,62.2}$) and total ventilation rate required by ASHRAE Standard 62.2-2016 ($Q_{tot,62.2}$). In the heating months (October to following March), the infiltration credit underestimated the infiltration rate by an average of 175 %. In cooling months, the infiltration credit underestimated the infiltration rate by an average of 95 %. Monthly average infiltration rates for Atlanta and Baltimore showed similar trends but are not presented here. It should be noted that at the NZERTF, the CONTAM$_{s,E}$ model predicted infiltration that is closest to the infiltration credit, though still higher than the credit in many months.

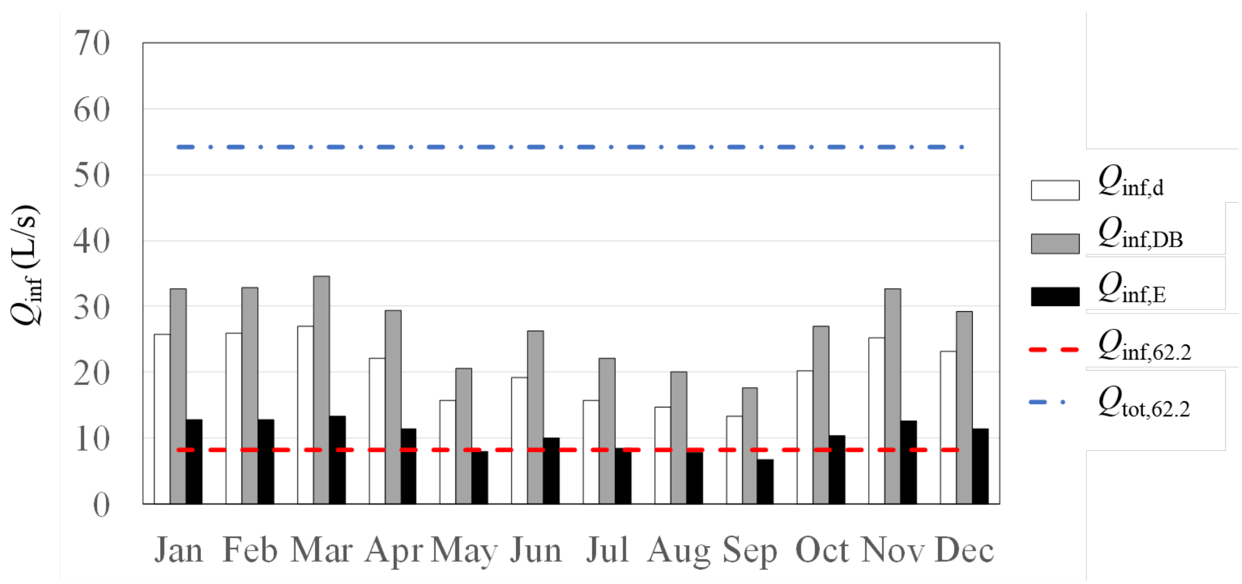

Fig. 12. Monthly average infiltration predicted by three CONTAM models in Chicago at the NZERTF. The horizontal lines show the infiltration credit and total outdoor airflow rate required by ASHRAE Standard 62.2-2016.

These findings of predicted infiltration rates below $Q_{inf,62.2}$ indicate that energy savings may be possible if RT control of an MV fan is implemented, especially during times when the infiltration rate was greater than $Q_{inf,62.2}$ or met $Q_{tot,62.2}$.

5.2. Average Q_{fan} flow rate

The average of $Q_{fan,RT}$ at the NZERTF predicted by the RT ventilation control strategies for all the cities (37 L/s) is larger than for the MH (8 L/s) for Scenario 1. The RT ventilation control strategies predicted an annual average $Q_{fan,RT}$ that was 38 % less than what is required by ASHRAE Standard 62.2-2016 at the MH, and 21 % less at the NZERTF when the fan-off flows were included. It should be noted that while the average $Q_{fan,RT}$ fan flow rate is less than what is required in the standard, the maximum fan airflow required in Scenario 1 is equal to $Q_{tot,62.2}$. This is to ensure that when the infiltration was close to zero, the total outdoor ventilation rate could still be met. It should also be noted that if fan-off flows were not included in the average, the annual average $Q_{fan,RT}$ at the MH would be 13 L/s across the three cities, which is a 7 % reduction from what is required by ASHRAE Standard 62.2-2016. Because the NZERTF requires more MV, its annual average $Q_{fan,RT}$ is not affected by the fan-off flows.

Fig. 13(a) shows that for the MH, the difference between the average $Q_{fan,RT\text{-}DB}$ and $Q_{fan,RT\text{-}E}$ was small (< 2 L/s) for Scenario 1. In Atlanta, the average $Q_{fan,RT}$ for all three of the RT ventilation control strategies were similar (3 % difference). However, in Baltimore and Chicago, the average $Q_{fan,RT\text{-}d}$ was the smallest among the three RT control strategies, 36 % and 71 % less, respectively, than $Q_{fan,RT\text{-}DB}$ and $Q_{fan,RT\text{-}E}$. These results indicate that a simplified CONTAM model was able to predict infiltration rates as well as a detailed CONTAM model in the mildest climate studied for the MH. The $Vent_{RT\text{-}DB}$ or $Vent_{RT\text{-}E}$ ventilation control strategies at the MH in the two colder cities tended to result in a conservative (low) estimate of the infiltration rates, and therefore overestimate the amount of mechanical ventilation needed compared with the fan size estimated for the $Vent_{RT\text{-}d}$ strategy.

Fig. 13(b) shows that for the NZERTF, the average $Q_{fan,RT\text{-}DB}$ and $Q_{fan,RT\text{-}E}$ were less similar than for the MH in Scenario 1. The average $Q_{fan,RT\text{-}E}$ was closer to the $Q_{fan,62.2}$ (4 % difference). The average $Q_{fan,RT\text{-}d}$ and $Q_{fan,RT\text{-}DB}$ were more similar to one another, but the average difference between the two was still 14 %. Contrary to the results at the MH, the $Q_{fan,RT\text{-}E}$ for the NZERTF was larger than the $Q_{fan,RT\text{-}d}$ and $Q_{fan,RT\text{-}DB}$. These findings may indicate that in a tight home like the NZERTF, it is not as clear which simplified model performs best based on the annual average flow rate of $Q_{fan,RT}$ in the three cities studied. Further, while LBNL's database used in the DB method included 147,000 homes, there were very few homes that were high-performance homes like the NZERTF. The majority of homes in ResDB had an *NL* between 0.2 and 2.0, whereas the *NL* of the NZERTF is 0.08. Further, Chan et al. [17] note that central estimates of *NL* are predicted with the equations in Sec. 3.1 and variability was estimated in their work to be substantial. Thus, tighter homes using the $Vent_{RT,DB}$ control strategy may overestimate infiltration rates when compared with the $Vent_{RT,d}$ control strategy. Nevertheless, the $Vent_{RT\text{-}E}$ control strategy provided a conservative (low) estimate of infiltration rates, and thus a higher $Q_{fan,RT\text{-}E}$ flow.

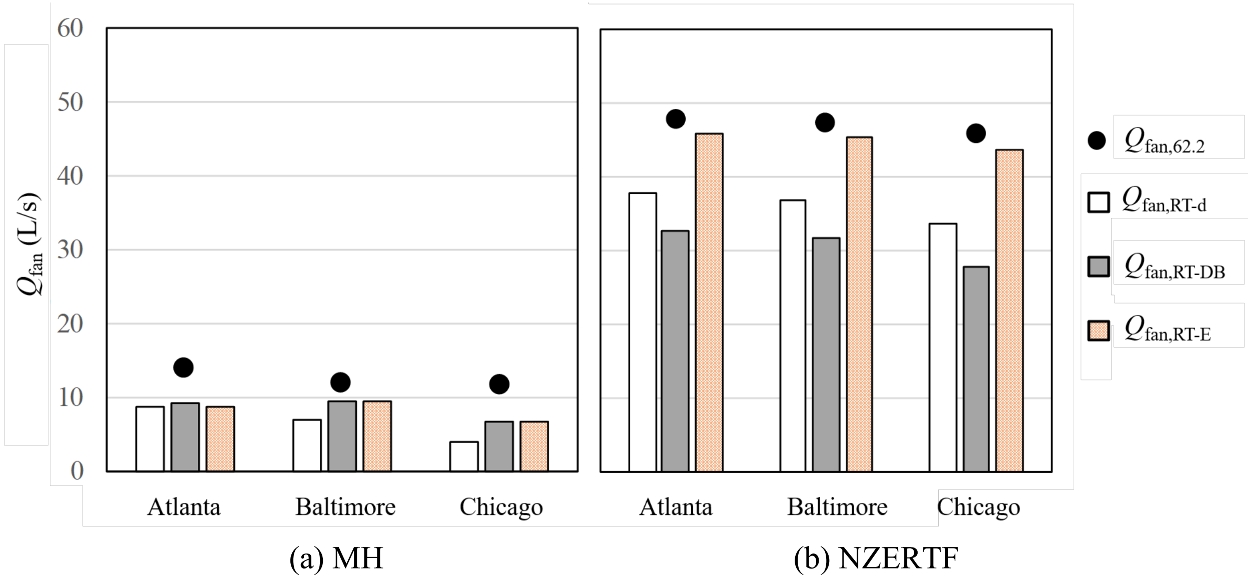

Fig. 13. Annual average $Q_{fan,RT}$ flow rate at (a) MH and (b) NZERTF for Scenario 1. $Q_{fan,62.2}$ is shown for reference.

5.3. Ventilation hours

Fig. 14 shows the number of hours when the total ventilation ($Q_{tot,62.2}$) was: (1) met by infiltration-alone; (2) met by infiltration plus mechanical ventilation; and (3) was unmet. The total of these hours is equal to 8760 h (i.e., one year). These graphs are for Scenario 1, where $Q_{fan,RT}$ was allowed to be greater than $Q_{fan,62.2}$. The results are shown for each city and the four ventilation control strategies.

Even though the MV fan ran continuously at a rate of $Q_{fan,62.2}$ for the Vent$_{cont}$ strategy, there were unmet ventilation hours when the predicted CONTAM$_d$ infiltration rate was less than $Q_{inf,62.2}$ (Fig. 14). Unmet ventilation hours can be eliminated with RT ventilation control strategies by allowing $Q_{fan,RT} > Q_{fan,62.2}$ to make-up for the times when infiltration was lower than the infiltration credit, such as for the Vent$_{RT\text{-}d}$, Vent$_{RT\text{-}DB}$, and Vent$_{RT\text{-}E}$ control strategies in Scenario 1. $Q_{tot,62.2}$ was unmet 24 % of the year (89 days) at the MH using the Vent$_{cont}$ strategy. At the NZERTF, it was unmet 10 % of the year (35 days) using the same ventilation strategy.

The most notable difference between Fig. 14a (MH) and Fig. 14b (NZERTF) is that in the MH there are more hours of the year where infiltration-alone met the ventilation requirement ($Q_{inf} \geq Q_{tot,62.2}$) than in the NZERTF. This is because the NZERTF is much tighter than the MH, thus the infiltration rates are lower. In addition, the NZERTF requires more ventilation because it is larger. As expected, the colder the climate, the greater the number of met-ventilation hours by infiltration-alone in both houses. The only RT ventilation strategy where infiltration-alone never met the ventilation requirement was for the Vent$_{RT\text{-}E}$ strategy at the NZERTF. In this strategy, the fan had to operate continuously because the predicted $Q_{inf,E}$ was very similar to the conservative infiltration credit (see Table 10) and MV was always required to meet $Q_{tot,62.2}$.

On average, $Q_{tot,62.2}$ was met by infiltration-alone at the MH across the three cities for almost half the year. At the NZERTF, ventilation was on average met by infiltration-alone only 2 % of the year. With MV, the three RT ventilation control strategies resulted in no unmet ventilation hours.

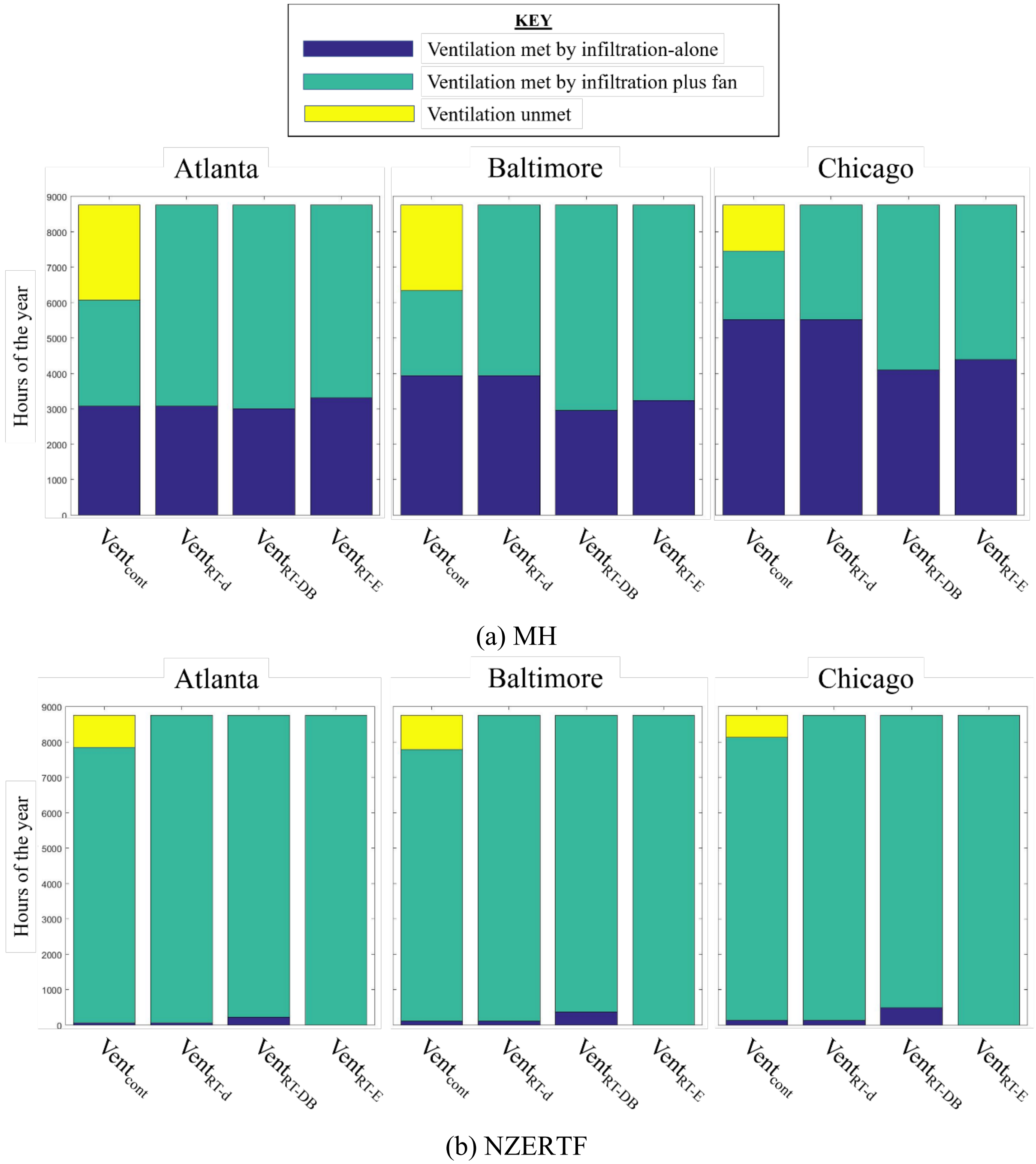

Fig. 14. Hours of the year $Q_{tot,62.2}$ met by infiltration-alone, met by MV plus infiltration, and unmet at (a) MH and (b) NZERTF for Scenario 1 where $Q_{fan,RT}$ allowed to exceed $Q_{fan,62.2}$.

For Scenario 2, when $Q_{\text{fan,RT}}$ was limited to be less than or equal to $Q_{\text{fan,62.2}}$, the number of unmet ventilation hours increased as expected (Fig. 15). Scenario 2 increased the number of unmet hours for the RT ventilation control strategies from zero to over 2600 hours (30 % of the year) across the three cities at the MH and to over 1600 hours (18 % of the year) at the NZERTF. Note that ASHRAE Standard 62.2-2016 does not have requirements related to unmet ventilation hours. It only requires non-continuous ventilation operation demonstrate that occupant exposure not increase above that which results from continuous ventilation operation.

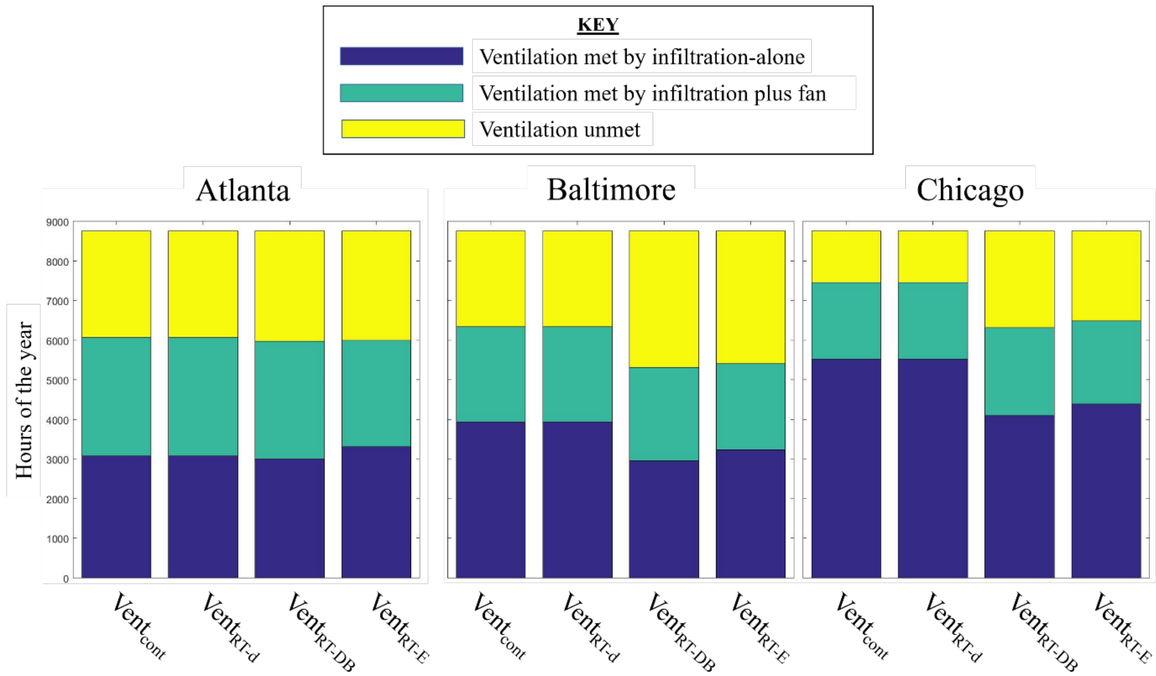

(a) MH

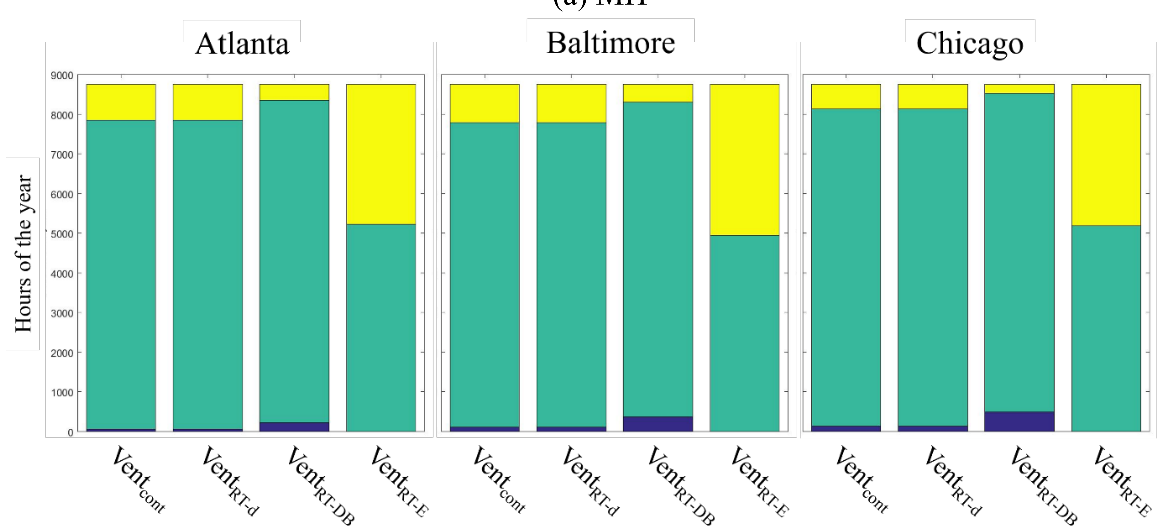

(b) NZERTF

Fig. 15. Hours of the year $Q_{\text{tot,62.2}}$ met by infiltration-alone, met by MV plus infiltration, and unmet at (a) MH and (b) NZERTF for Scenario 2 where $Q_{\text{fan,RT}} \le Q_{\text{fan,62.2}}$.

5.4. Relative exposure factor

Table 11 and Table 12 show the annual relative exposure factor (R_{avg}) for the three RT ventilation control strategies across the three cities for both test houses and both fan-sizing scenarios. The annual relative exposure factor of the RT ventilation strategies was less than or equal to 1.0 for both test houses in all three cities for both fan-sizing scenarios. The highest R_{avg} values were at the NZERTF. Table 11 and Table 12 show that despite the limitation on $Q_{fan,RT}$ in Scenario 2, the increase in average R_{avg} was only 8 % at the MH and 1 % at the NZERTF. At the NZERTF, this increase is not apparent in Table 12 because the values in the table are only shown to two significant figures.

There were no hours of the year at the MH or the NZERTF when R_i was greater than 5.0, which is the limit in ASHRAE Standard 62.2-2016. The findings of reduced average $Q_{fan,RT}$ in Sec. 5.2 and the relatively small impact on R_{avg} indicate that potential energy savings may be realized with reduced fan operation, while not significantly increasing occupant exposure. On the contrary, at the MH, R_{avg} per the exposure assumed in this study was reduced with RT ventilation control compared with continuous ventilation at $Q_{tot,62.2}$. At the NZERTF, R_{avg} RT ventilation control remained similar to the exposure using continuous ventilation at $Q_{tot,62.2}$. Therefore, based on the RT ventilation control strategies studied, users of ASHRAE Standard 62.2-2016 could install the fan size specified in the standard (i.e., Scenario 2 where $Q_{fan} = Q_{fan,62.2}$) with insignificant increases in relative occupant exposure over a year compared with installing a fan sized to deliver $Q_{tot,62.2}$ (i.e., Scenario 1).

Table 11. R_{avg} at MH in three cities.

RT ventilation control strategy	MH					
	Scenario 1			Scenario 2		
	Atlanta	Baltimore	Chicago	Atlanta	Baltimore	Chicago
$Vent_{RT,d}$	0.9	0.8	0.7	0.9	0.9	0.8
$Vent_{RT,DB}$	0.9	0.9	0.8	0.9	1.0	0.9
$Vent_{RT,E}$	0.9	0.8	0.8	0.9	0.9	0.8
Average		0.8		0.9 (13 % increase relative to Scenario 1[a])		

[a]It should be noted that the difference is reported as 13 % based on the number of significant digits reported. If more significant digits were considered, the difference would be 8 %.

Table 12. R_{avg} at NZERTF in three cities.

RT ventilation control strategy	NZERTF					
	Scenario 1			Scenario 2		
	Atlanta	Baltimore	Chicago	Atlanta	Baltimore	Chicago
$Vent_{RT,d}$	1.0	1.0	1.0	1.0	1.0	1.0
$Vent_{RT,DB}$	1.0	1.0	1.0	1.0	1.0	1.0
$Vent_{RT,E}$	1.0	1.0	1.0	1.0	1.0	1.0
Average		1.0			1.0 (0 % increase relative to Scenario 1[a])	

[a]It should be noted that the difference is reported as 0 % based on the number of significant digits reported. If more significant digits were considered, the difference would be 1 %.

5.5. Energy impacts of ventilation

As outlined in Sec. 4.5, the energy required for ventilation is evaluated in this study in terms of: (1) the energy to operate the mechanical ventilation (MV) fan, (2) the sensible energy to condition the MV air, and (3) the sensible energy to condition the infiltration air. It was assumed that the MV system did not have heat recovery. The energy required was then converted to energy cost using an assumed cost of electricity per kilowatt-hour (kWh). In order to understand the energy impacts, a discussion of fan runtimes is presented first.

Fig. 16 presents the percentage reduction in fan runtime of the RT ventilation control strategies compared with the more typical case of continuous fan operation (i.e., the $Vent_{cont}$ strategy). Fig. 16 shows that at the MH, there was an average 43 % reduction in fan runtime across the three cities for the three RT control strategies. At the NZERTF, the average fan runtime reduction was only 2 %. The reduction was greater in the MH because it is leakier and subsequently, infiltration-alone could fulfill the ventilation requirement more of the time. In the tighter NZERTF, the $Vent_{RT\text{-}DB}$ strategy shows a greater reduction in fan runtime compared with the $Vent_{RT\text{-}d}$ strategy due to the $CONTAM_{s,DB}$ model estimating a higher average infiltration than the $CONTAM_{d}$ model. At the NZERTF, the $CONTAM_{RT\text{-}E}$ model predicted the lowest infiltration rate, thus the fan needed to run continuously under the $Vent_{RT\text{-}E}$ strategy and there was no reduction in fan runtime. The fan runtime reduction varied from 1 % to 63 % across all RT ventilation control strategies, cities and houses, and so all control strategies provided some level of energy savings as compared with the $Vent_{cont}$ strategy.

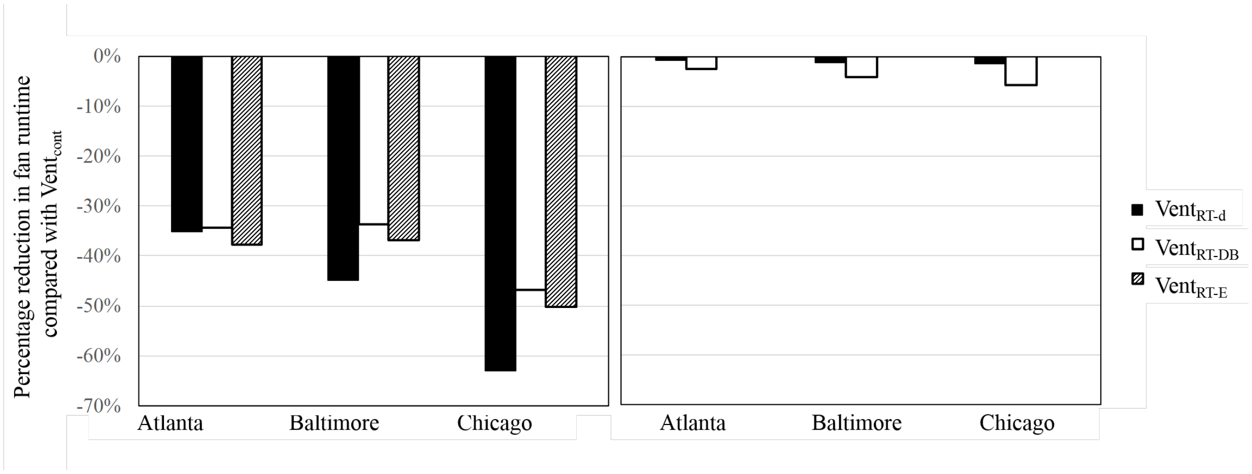

(a) MH (b) NZERTF

Fig. 16. Percentage reduction in fan runtime for RT control strategies at (a) MH and (b) NZERTF in three cities compared with Vent$_{cont}$ strategy.

Fig. 17 shows the cost difference of implementing each RT ventilation control strategy compared with the Vent$_{cont}$ strategy for fan-sizing Scenario 1. The cost differences are calculated for both test houses, in each city, and split into to the differences resulting from (1) conditioning the MV air, (2) operating the MV fan, and (3) conditioning the infiltration air. Fig. 17 shows that for the Vent$_{RT,d}$ strategy (both homes, all cities), there are no savings from conditioning the infiltration air because the infiltration used in the Vent$_{cont}$ and Vent$_{RT,d}$ strategies were both from the CONTAM$_d$ model. In all RT ventilation strategies, the smallest savings came from reducing the MV fan operation. There was also a trend that in the coldest city of those studied, i.e., Chicago, the total energy (operation and conditioning) cost savings was the greatest.

At the MH (Fig. 17a), the RT ventilation strategies predicted savings from conditioning the infiltration air that were greater than the savings from conditioning the MV air, except in Atlanta. In Atlanta, the savings from conditioning the MV air were about the same as the savings from conditioning the infiltration air. Of the three RT ventilation strategies and across the three cities, the total annual energy cost savings at the MH ranged from \$36 to \$98 (average = \$57). For Scenario 2, when the fan flow rate was limited to be less than or equal to $Q_{fan,62.2}$, the total energy savings increased to \$42 to \$109 (average = \$67) a year across the three cities at the MH.

At the NZERTF (Fig. 17b), the Vent$_{RT,DB}$ strategy showed an increase in energy cost required to condition infiltration air in all three cities when compared with conditioning the infiltration air supplied by CONTAM$_d$ in the Vent$_{cont}$ strategy. This is due to the modeled infiltration of the CONTAM$_{s,DB}$ model being greater than the CONTAM$_d$ infiltration rates. Nevertheless, the increase in energy cost was offset by the savings in MV fan operation and in conditioning the MV air. For the three RT ventilation strategies, the total annual energy cost savings at the NZERTF ranged from \$44 to \$113 (average = \$78) for Scenario 1. For Scenario 2, when the fan flow rate was limited to be less than or equal to $Q_{fan,62.2}$, the range of total energy cost savings increased very little to \$47 to \$114 (average = \$80). This change is small because the ASHRAE Standard 62.2-2016 fan flow requirement is higher for the NZERTF compared with the MH, and when limits were placed on $Q_{fan,RT}$, it affected the NZERTF less because the average predicted fan flow rate was already closer to $Q_{fan,62.2}$ at the NZERTF.

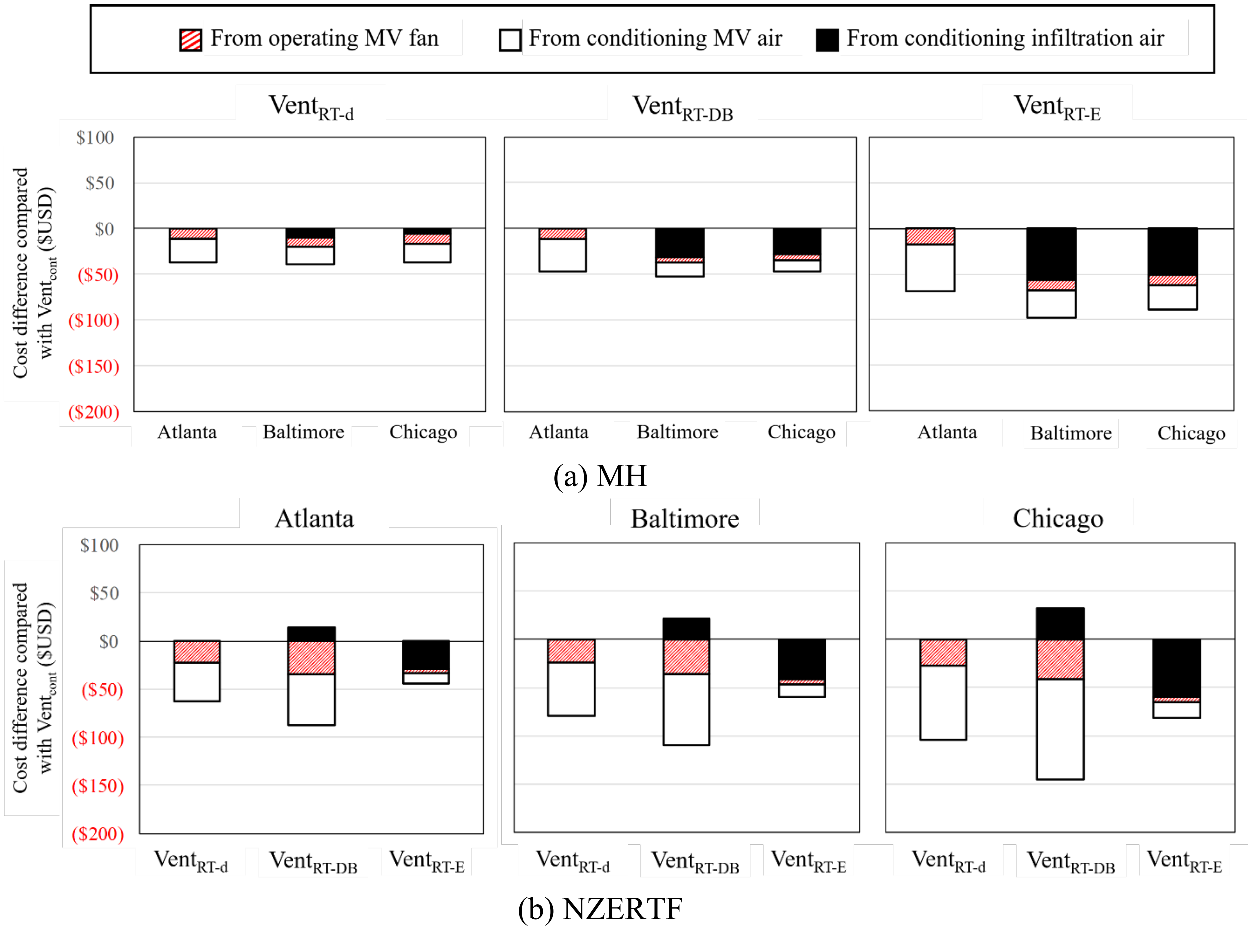

Fig. 17. Energy cost difference for fan-sizing Scenario 1 at (a) MH and (b) NZERTF.

It should be noted that the cost to condition the infiltration air predicted by the three CONTAM models was 2 to 5 times higher than the cost to condition the infiltration rate based on the ASHRAE Standard 62.2-2016 infiltration credit throughout the year. As discussed in Sec. 5.1, this is due to the fact that the average predicted infiltration was higher than the ASHRAE Standard 62.2-2016 infiltration credit in both test houses and in all the cities studied.

6. Discussion and Limitations

In this study, the authors studied the performance of RT ventilation control strategies using detailed and simplified CONTAM models to predict hourly infiltration rates and incorporating them into a theoretical controller. Four ventilation control strategies were evaluated at the MH and NZERTF, three of which were RT control strategies using results of different CONTAM models for estimating infiltration.

When using CONTAM models to predict RT infiltration for fan-sizing under Scenario 1, as opposed to assuming a constant infiltration rate, we found an average 29 % reduction in the average MV airflow compared with the requirement in ASHRAE Standard 62.2.-2016 for the two test houses and three cities studied. This was when fan-off flow rates were also included in the average. When fan-off flow rates were excluded from the average, the reduction in MV across the two test houses and three cities was 6 %. In Scenario 2, when the fan flow rate was limited to the requirement in the standard, there was an average reduction of 39 % in the average MV airflow compared with the standard's requirement. However, the greater reduction in MV flow increased the number of unmet ventilation hours to over 2000 h (or 88 days) under Scenario 2. For all RT control strategies and in all cities, reducing the average MV airflow did not increase annual relative exposure above the limits in the standard. The RT control strategies resulted in an average annual savings of $68 across both test houses and three cities for Scenario 1. For Scenario 2, the average annual savings was $73. While the savings in an individual home may not seem large, across a larger community of homes, the total savings would be more substantial.

Each of the RT ventilation control strategies had advantages and disadvantages. The $Vent_{RT,d}$ strategy used infiltration rates from a verified, detailed CONTAM model of the house. However, developing and verifying the detailed model required expertise and time. Both the $Vent_{RT,DB}$ and $Vent_{RT,E}$ control strategies used infiltration rates from a single-zone model, requiring only the building height, volume, a weather file, orientation, and exterior envelope leakage area. Many of these could be obtained from the homeowner or estimated from other data sources such as satellite imagery. Note that the real-time weather needed for RT ventilation control is currently available via a range of mechanisms and is are already applied in many smart thermostats.

The advantage of the $Vent_{RT,DB}$ control strategy is that no measurements are required to obtain the exterior envelope leakage area. This control strategy utilizes existing leakage-area correlations, with the inputs including year of construction and foundation type. While LBNL's database for these correlations includes 147,000 homes, there were very few homes that were high-performance homes like the NZERTF. Thus, tighter homes using the $Vent_{RT,DB}$ control strategy may overestimate infiltration rates when compared with the $Vent_{RT,d}$ control strategy. The $Vent_{RT,E}$ control strategy did require measurements. However, it used existing kitchen exhaust fans, which is simpler than blower door testing, but also required differential pressure transducers that are accurate at low pressures. While the use of differential pressure transducers requires a measurement across the building envelope (e.g., through a window opening), it is only required for the duration of the exhaust fan tests.

7. Future work

Additional measurement and simulation exercises would be useful to achieve a better understanding of the performance of RT ventilation controllers using infiltration rates estimates. In particular, the test houses are examples of particularly tight and leaky construction; it would be useful to evaluate homes that are more typical in terms of envelope airtightness. The analyses also assumed that the MV system was balanced. However, other types of ventilation systems should be evaluated, such as exhaust-only, supply-only, and those integrated with the heating/cooling system.

Estimating envelope leakage from an exhaust fan test shows promise when a full blower-door test is not the preferred option. The exhaust fan tests conducted in this study yielded reasonable results at both the MH and NZERTF, but more homes should be tested to see how the results compare to standard blower doors tests. Based on additional tests, it may be possible to develop a standardized test procedure for local exhaust fan airtightness tests for residential buildings.

When evaluating the impacts of outdoor air ventilation on energy, only sensible heat was considered in this study. The impact of latent heat load on a home, especially in summer, needs to be considered, particularly for cities like Atlanta, where the latent load could exceed the sensible load. For this type of analysis, a coupled airflow-energy model is ideal, such as the CONTAM-EnergyPlus model used here [26, 40].

The simplified CONTAM model used in two of the RT ventilation control strategies was created manually. Automating the process and embedding it onto a microprocessor for integration into HVAC equipment control could greatly facilitate the application of RT ventilation control. Other capabilities could also be added to the microprocessor, such as collecting weather data, outdoor air quality and user inputs about a home to further facilitate the application of real-time ventilation control strategies.

There may also be methods to estimate real-time infiltration that would not rely on a CONTAM model, such as regression models, artificial intelligence, or a combination of CONTAM simulations and data-driven models. These approaches would require more measurements to be taken in more houses and in more locations. There are also other models of infiltration, such as the AIM-2 [9] that can be used to estimate infiltration and may be easier to program into a controller than CONTAM.

This study evaluated occupant exposure using a uniformly-distributed, constant and generic contaminant source as outlined in ASHRAE Standard 62.2-2016. In reality, airborne contaminant sources exhibit spatial and temporal variation, and have very different health and comfort impacts on building occupants. With the increased availability of consumer-grade air monitors and the continual improvement in their measurement accuracy, it may be possible to implement ventilation control that is more responsive to individual indoor environments and to the occupants' unique health and comfort needs and preferences.

8. Conclusions

Outdoor air ventilation rates specified in ASHRAE Standard 62.2-2016 account for infiltration using a single, constant value. However, infiltration rates vary significantly with ventilation system operation, weather, and indoor conditions in accordance with known physical relationships. Thus, a single assumed or measured infiltration rate may not be appropriate when determining whether the total outdoor air ventilation rate requirement is met throughout the year. The authors proposed the use of CONTAM airflow models to determine real-time infiltration rates, which could then be passed to an RT ventilation system controller to reduce or eliminate MV when the infiltration is greater than the credit assigned per ASHRAE Standard 62.2-2016. The method was evaluated for two test houses on the NIST campus in Gaithersburg, MD, USA. The implementation of the theoretical controller resulted in predicted annual energy cost savings ranging from $36 to $98 (average = $57) in the MH and $44 to $113 (average = $78) in the NZERTF. These savings were realized without a significant increase in annual occupant exposure to a simple, generic contaminant, relative to ventilating continuously at a single rate. In many cases, the annual occupant exposure improved with RT ventilation control.

Acknowledgements

The authors would like to thank Jonathan Wilson and David Jacobs from the National Center for Healthy Housing for partially funding this research in conjunction with Beetle Management, Inc under CRADA CN-17-0080. The authors would also like to thank Gabriel Grajewski and Daniel Greb at NIST for their key contributions to the experimental efforts.

References

[1] ASHRAE (2016)– *ASHRAE Standard 62.2-2016: Ventilation and Acceptable Indoor Air Quality in Low-Rise Residential Buildings* (American Society of Heating, Refrigerating and Air-Conditioning Engineers, Inc., Atlanta).

[2] Persily AK , Martin SR (2000) A Modeling Study of Ventilation in Manufactured Houses. (National Institute of Standards and Technology, Gaithersburg), NISTIR 6455, February 2000.

[3] Guyot G, Sherman MH, Walker IS (2018) Smart ventilation energy and indoor air quality performance in residential buildings: A review. *Energ Buildings* 165:416-430. https://doi.org/10.1016/j.enbuild.2017.12.051

[4] Martin E, Fenaughty K, Parker D, Lubliner M, Howard L (2018) Field and Laboratory Testing of Approaches to Smart Whole-House Mechanical Ventilation Control. (National Renewable Energy Laboratory (NREL), Golden, CO). https://doi.org/https://doi.org/10.2172/1416954

[5] Hesaraki A , Holmberg S (2015) Demand-controlled ventilation in new residential buildings: Consequences on indoor air quality and energy savings. *Indoor and Built Environment* 24(2):162-173. https://doi.org/10.1177/1420326x13508565

[6] Turner WJN , Walker IS (2012) Advanced Controls and Sustainable Systems for Residential Ventilation. (Lawrence Berkeley National Laboratory, Berkeley, CA). https://doi.org/http://escholarship.org/uc/item/7wq1z8w9

[7] Sherman MH , Walker IS (2011) Meeting residential ventilation standards through dynamic control of ventilation systems. *Energ Buildings* 43(8):1904-1912. https://doi.org/10.1016/j.enbuild.2011.03.037

[8] Walker IS , Less BB (2018) Rethinking Occupancy-Based Ventilation Controls. *39th AIVC Conference 2018*, (Air Infiltration and Ventilation Centre, Juan-les-Pins, France).

[9] Walker IS , Wilson DJ (1990) The Alberta Air Infiltration Model. (Unversity of Alberta, Alberta, Canada).

[10] Less BD (2019) Personal communication regarding infiltration estimation methods in "Rethinking Occupancy-Based Ventilation Controls" in 39th AIVC Conference 2018. ed Ng L.

[11] Clark JD, Less BD, Dutton SM, Walker IS, Sherman MH (2019) Efficacy of occupancy-based smart ventilation control strategies in energy-efficient homes in the United States. *Build Environ*. https://doi.org/10.1016/j.buildenv.2019.03.002

[12] Dols WS, Emmerich SJ, Polidoro BJ (2016) Coupling the multizone airflow and contaminant transport software CONTAM with EnergyPlus using co-simulation. *Building Simulation* 9:469-479. https://doi.org/10.1007/s12273-016-0279-2
[13] Persily AK (2016) Field measurement of ventilation rates. *Indoor Air* 26(1):97-111. https://doi.org/http://dx.doi.org/10.1111/ina.12193
[14] ASTM (2011)– *ASTM E741-11 Standard Test Method for Determining Air Change in a Single Zone by Means of a Tracer Gas Dilution* (American Society for Testing and Materials, West Conshohocken, PA).
[15] ASTM (2010)– *ASTM E779-10 Standard Test Method for Determining Air Leakage Rate by Fan Pressurization* (American Society of Testing and Materials, Philadelphia).
[16] Chan WR, Joh J, Sherman MH (2013) Analysis of air leakage measurements of US houses. *Energ Buildings* 66(0):616-625. https://doi.org/http://dx.doi.org/10.1016/j.enbuild.2013.07.047
[17] Chan WR, Joh J, Sherman MH (2013) Analysis of Air Leakage Measurements from Residential Diagnostics Database. (Lawrence Berkeley National Laboratory, Berkeley, CA).
[18] Dols WS , Polidoro B (2016) CONTAM User Guide and Program Documentation. (National Institute of Standards and Technology, Gaithersburg, MD), Technical Note 1887.
[19] Haghighat F , Megri AC (1996) A Comprehensive Validation of Two Airflow Models - COMIS and CONTAM. *Indoor Air* 6(4):278-288.
[20] Chung KC (1996) Development and validation of a multizone model for overall indoor air environment prediction. *HVAC&R Res* 2(4):376-385.
[21] Emmerich SJ, Nabinger SJ, Gupte A, Howard-Reed C (2004) Validation of multizone IAQ model predictions for tracer gas in a townhouse. *Building Services Engineering Research and Technology* 25(4):305-316.
[22] Emmerich SJ (2001) Validation of Multizone IAQ Modeling of Residential-Scale Buildings: A Review. *ASHRAE Tran* 107(2):619-628.
[23] Nabinger S , Persily A (2011) Impacts of airtightening retrofits on ventilation rates and energy consumption in a manufactured home. *Energ Buildings* 43(11):3059-3067. https://doi.org/10.1016/j.enbuild.2011.07.027
[24] Nabinger S , Persily A (2008) Airtightness, Ventilation and Energy Consumption in a Manufactured House: Pre-Retrofit Results. (NIST, Gaithersburg, MD).
[25] Pettit B, Gates C, Fanney AH, Healy W (2014) Design Challenges of the NIST Net-Zero Energy Residential Test Facility. (National Institute of Standards and Technology, Gaithersburg, MD).
[26] Fanney AH, Payne V, Ullah T, Ng L, Boyd M, Omar F, Davis M, Skye H, Dougherty B, Polidoro B, Healy W, Kneifel J, Pettit B (2015) Net-zero and beyond! Design and performance of NIST's Net-Zero Energy Residential Test Facility. *Energ Buildings* 101(0):95-109. https://doi.org/http://dx.doi.org/10.1016/j.enbuild.2015.05.002
[27] Fanney H, Healy WM, Payne V, Kneifel J, Ng L, Dougherty BP, Ullah T, Omar F (2017) Small Changes Yield Large results at NIST's Net-Zero Energy Residentail Test Facility. *Journal of Solar Energy Engineering*. https://doi.org/10.1115/1.4037815

[28] NREL (2015) *National Solar Radiation Data Base - 1991-2005 Update: Typical Meteorological Year 3*. Available at http://rredc.nrel.gov/solar/old_data/nsrdb/1991-2005/tmy3/.

[29] Ng L, Poppendieck D, Dols WS, Emmerich SJ (2017) Evaluating indoor air quality and energy impacts of ventilation in a net-zero energy house using a coupled model. *Science and Technology for the Built Environment* 24(2):124-134. https://doi.org/https://doi.org/10.1080/23744731.2017.1401403

[30] Persily A, Musser A, Emmerich SJ (2010) Modeled infiltration rate distributions for U.S. housing. *Indoor Air* 20(6):473-485. https://doi.org/10.1111/j.1600-0668.2010.00669.x

[31] ASHRAE (2017)– *ASHRAE Handbook Fundamentals* (American Society of Heating, Refrigerating and Air-Conditioning Engineers, Atlanta).

[32] Sherman MH (1992) Single-Zone Stack-Dominated Infiltration Modeling (Lawrence Berkeley National Laboratory, Berkeley, CA).

[33] Ng L, Persily A, Emmerich S (2015) Infiltration and Ventilation in a Very Tight, High Performance Home. *36th AIVC Conference Effective Ventilation in High Performance Buildings*, pp 719-726.

[34] Modera M, P. , Sherman M, H. , Grimsrud D, T. (1982) A Predictive Air Infiltration Model—Long-Term Field Test Validation. *ASHRAE Tran* 88(1).

[35] Modera M, P., Sherman M, H. , Levin PA (1983) A Detailed Examination of the LBL Infiltration Model with the Mobile Infiltration Test Unit. *ASHRAE Tran* 89.

[36] Sherman MH , Modera MP (1986) *Comparison of Measured and Predicted Infiltration Using the LBL Infiltration Model* (ASTM International, West Conshohocken, PA), pp 325-347.

[37] HVI (2019) HVI-Certified Products Directory. (Home Ventilating Institute, Phoenix, AZ).

[38] AHRI (2019) AHRI Certification Directory. (Air-Conditioning, Heating and Refrigeration Institute, Arlington, VA).

[39] EIA (2018) Short-Term Energy Outlook (STEO). (U. S. Energy Information Administration, Washington, D.C.).

[40] Dols WS, Emmerich SJ, Polidoro BJ (2015) Using coupled energy, airflow and indoor air quality software (TRNSYS/CONTAM) to evaluate building ventilation strategies. *Building Services Engineering Research and Technology* 37(2):163-175. https://doi.org/doi: 10.1177/0143624415619464